Atmos. Chem. Phys. Discuss., https://doi.org/10.5194/acp-2018-920
Manuscript under review for journal Atmos. Chem. Phys.
Discussion started: 17 October 2018
© Author(s) 2018. CC BY 4.0 License.

Atmospheric Chemistry and Physics Discussions

Effects of two different biogenic emission models on modelled ozone and aerosol concentrations in Europe

Jianhui Jiang[1], Sebnem Aksoyoglu[1], Giancarlo Ciarelli[2], Emmanouil Oikonomakis[1], Imad El-Haddad[1], Francesco Canonaco[1], Colin O'Dowd[3,4], Jurgita Ovadnevaite[3,4], María Cruz Minguillón[5], Urs Baltensperger[1], and André S. H. Prévôt[1]

[1]Laboratory of Atmospheric Chemistry, Paul Scherrer Institute, 5232 Villigen PSI, Switzerland
[2]Laboratoire Inter-Universitaire des Systèmes Atmosphériques (LISA), UMR CNRS 7583, Université Paris Est Créteil et Université Paris Diderot, Institut Pierre Simon Laplace, Créteil, France
[3]School of Physics, Centre for Climate and Air Pollution Studies, Ryan Institute, National University of Ireland Galway, University Road, H91CF50 Galway, Ireland
[4]Marine and Renewable Energy Ireland
[5]Institute of Environmental Assessment and Water Research (IDAEA), CSIC, 08034 Barcelona, Spain

Correspondence to: Sebnem Aksoyoglu (sebnem.aksoyoglu@psi.ch), Jianhui Jiang (jianhui.jiang@psi.ch)

Abstract. Biogenic volatile organic compound (BVOC) emissions are one of the essential inputs for chemical transport models (CTMs), but their estimates are associated with large uncertainties leading to significant influences on air quality modelling. This study aims at investigating the effects of using different BVOC emission models on the performance of a CTM in simulating secondary pollutants, i.e. ozone, organic and inorganic aerosols. The European air quality was simulated for the year 2011 by the regional air quality model Comprehensive Air Quality Model with Extensions (CAMx) version 6.3, using BVOC emissions calculated by two emission models: the Paul Scherrer Institute (PSI) model and the Model of Emissions of Gases and Aerosol from Nature (MEGAN) v2.1. Comparison of isoprene and monoterpene emissions from both models showed large differences in their general amounts as well as their spatial distribution both in summer and winter. MEGAN produced more isoprene emissions by a factor of 3 while the PSI model generated three times of monoterpene emissions in summer, while there was negligible difference (~4%) in sesquiterpene emissions associated with the two models. Despite the large differences in isoprene emissions (i.e. 3-fold), the resulting impact in predicted summer-time ozone proved to be minor (<10%, O_3-MEGAN was higher than O_3-PSI by ~7 ppb). Comparisons with measurements from the European air quality database (AirBase) indicated that PSI emissions might improve the model performance at low ozone concentrations, but worsen it at high ozone levels (>60 ppb). A much larger effect of the different BVOC emissions was found for the secondary organic aerosol (SOA) concentrations. The higher monoterpene emissions (a factor of ~3) by the PSI model led to higher SOA by ~110% on average in summer, compared to MEGAN, improving substantially the model performance for organic aerosol (OA): the mean bias between modelled and measured OA at 8 Aerodyne aerosol chemical speciation monitor (ACSM)/Aerodyne aerosol mass spectrometer (AMS) measurement stations was reduced by 21% – 83% in rural/remote stations. Effects on inorganic aerosols (particulate nitrate, sulphate, and ammonia) were relatively smaller (< 15%).

Atmos. Chem. Phys. Discuss., https://doi.org/10.5194/acp-2018-920
Manuscript under review for journal Atmos. Chem. Phys.
Discussion started: 17 October 2018
© Author(s) 2018. CC BY 4.0 License.

Atmospheric Chemistry and Physics Discussions

1 Introduction

Biogenic volatile organic compounds (BVOCs) from the terrestrial biosphere play an important role in atmospheric chemistry. They affect ozone production strongly (Calfapietra et al., 2013; Curci et al., 2009) and are the largest source of secondary organic aerosol (SOA) worldwide (Bonn et al., 2004; Hallquist et al., 2009; Hodzic et al., 2016). Emissions of BVOCs such as isoprene, monoterpenes (MT) and sesquiterpenes (SQT) are now commonly used as inputs within numerous chemical transport models (CTMs). While in many model inter-comparison studies anthropogenic emissions are harmonized, biogenic emissions usually differ (Bessagnet et al., 2016; Colette et al., 2017; Solazzo et al., 2012). Different approaches in biogenic emission models may result in substantial difference on predicted emission rates of BVOCs (Messina et al., 2016; Oderbolz et al., 2013). Understanding the potential influence of biogenic VOC emission inputs on air quality model results is therefore of great importance to improve the performance of the CTMs.

BVOCs, dominated by isoprene and monoterpenes, are generated from biosynthesis of precursor isopentenyl pyrophosphate in plants (Kesselmeier and Staudt, 1999). Isoprene is emitted from leaf surfaces immediately after synthesis (referred to as synthesis emission), while monoterpenes are mostly stored in plant organs after their production (pool emission) and some monoterpene species have synthesis emissions as well. The synthesis and emission processes could be influenced by various factors, such as plant species, foliage biomass, temperature, solar radiation as well as carbon and water availability (Grote and Niinemets, 2008), leading to high uncertainty in the estimates of BVOC emissions. Current BVOC emission models are mostly based on an empirical bottom-up approach by emission factors as a function of leaf temperature and photosynthetically active radiation (PAR) (Andreani-Aksoyoglu and Keller, 1995; Guenther et al., 2006; Guenther et al., 2012; Solmon et al., 2004). Although most of these models share similar algorithms, the inputs such as emission factors and land use types might vary widely for different studies. For example, the widely used MEGAN (Model of Emissions of Gases and Aerosols from Nature) (Guenther et al., 2012) estimates 19 categories of BVOC species by emission factors based on 15 CLM4 (Community Land Model) plant function types (PFT) (e.g., broadleaf evergreen tropical tree, broadleaf deciduous temperate shrub, etc.). To account for variability of different tree species within the same PFT, MEGAN2.1 provides emission factors for more than 2000 ecoregions worldwide based on tree species composition and tree-species-specific emission factors (Guenther et al., 2012). For regional simulations in which more detailed land use and vegetation information were available, Solmon et al. (2004) estimated isoprene and monoterpenes emissions in France based on Corine Land Cover (CLC) land use data with a resolution of 50 – 100 m and BVOC emission factors of each tree species. Significant influences of land use and vegetation on the spatial distribution and magnitude of estimated BVOC emissions have been reported by many studies (Hantson et al., 2017; Oderbolz et al., 2013; Rosenkranz et al., 2015; Steinbrecher et al., 2009; Szogs et al., 2017).

As an important input to air quality models, BVOC emissions strongly influence simulated concentration of ozone and aerosols. BVOCs play crucial roles in both formation and removal processes of ozone (Calfapietra et al., 2013). Comparison between MEGAN and another widely used biogenic emission model, the Biogenic Emission Inventory System (BEIS) indicated that the influence of biogenic emission models on ozone simulation results is among the highest over all the model inputs (Kim et al., 2017; Zhang et al., 2017). The potential influence of biogenic emissions on aerosol modelling results is more complicated. BVOCs are oxidized by reactions with oxidants like hydroxyl radicals (OH), nitrate radicals (NO_3) and ozone (O_3), and

© Author(s) 2018. CC BY 4.0 License.

generate secondary organic aerosols via gas-to-particle partitioning (Griffin et al., 1999; Hoffmann et al., 1997). Different estimates of BVOC emissions directly influence the amount of biogenic SOA precursors (mainly MTs and SQTs) (Bonn et al., 2004), while they also influence indirectly the aerosol simulations via effects on oxidants (Ayres et al., 2015; Calfapietra et al., 2013; Ng et al., 2017). Significant influence of anthropogenic activities and climate conditions on biogenic SOA formation (Carlton et al., 2010; Fu et al., 2014; Hoyle et al., 2011) makes it even more challenging to understand the effect of BVOC emissions on SOA simulations. The chemical reactions of BVOCs and their effects on oxidant concentrations also lead to significant changes in the formation of secondary inorganic aerosol, especially ammonium nitrate (Aksoyoglu et al., 2017).

In this study, we investigated the effects of different estimates of BVOC emissions on modelled ozone and aerosol concentrations in Europe. Biogenic emissions were estimated by two BVOC emission models with different land cover inputs and emission factors and then used in a whole-year simulation of gaseous and particulate pollutants in 2011 by the regional air quality model Comprehensive Air Quality Model with extensions (CAMx). The modelled results were then evaluated by comparisons with European air quality database AirBase and Aerodyne aerosol chemical speciation monitor (ACSM)/Aerodyne aerosol mass spectrometer (AMS) measurements.

2 Method and data

2.1 Regional air quality model CAMx

The regional air quality model CAMx version 6.3 (http://www.camx.com/) with the VBS (volatility basis set) scheme (Koo et al., 2014) was used to simulate the year 2011 in this study. The model domain (15^{o}W - 35^{o}E, 35^{o}N - 70^{o}N) covered Europe with a horizontal resolution of 0.25^{o} × 0.125^{o}. The meteorological inputs were prepared by the Weather Research and Forecasting Model WRF-ARW (Advanced Research WRF) version 3.7.1 (NCAR, 2016; Skamarock et al., 2008). We used the ECMWF (European Centre for Medium-Range Weather Forecasts) global atmospheric reanalysis ERA-Interim data as initial and boundary conditions for the WRF model, with a spatial resolution of 0.72^{o} × 0.72^{o} and a time step of 6 hours (Dee et al., 2011). The meteorological fields from the WRF output were further processed by WRF-CAMx version 4.4 (http://www.camx.com/download/support-software.aspx) to match the CAMx vertical layers and to prepare the required parameters (e.g. vertical diffusivity). In CAMx, there were 14 terrain-following vertical layers reaching up to 460 hPa, with the first layer being ~20 m thick. The Carbon Bond 6 Revision 2 (CB6r2) mechanism (Hildebrandt Ruiz and Yarwood, 2013) was used for the gas-phase chemistry. Aqueous sulphate and nitrate formation in resolved cloud water was simulated by the RADM algorithm (Chang et al., 1987). Partitioning of inorganic aerosol components between the gas and particle phases was calculated by the ISORROPIA thermodynamic model (Nenes et al., 1998). Organic aerosol formation from anthropogenic (including both land and ships) and biogenic (terrestrial) sources was modeled by the 1.5-D VBS organic aerosol chemistry/partitioning module (Koo et al., 2014), which describes the evolution of OA in the 2-D space of oxidation state and volatility. The standard CAMx v6.3 treats the aging and partitioning processes of secondary aerosols from biogenic and biomass burning sources in the same basis sets. To distinguish the contributions of biogenic and biomass burning sources to OA, we separated the combined basis set VBS/PBS (V – Vapor, P –

© Author(s) 2018. CC BY 4.0 License.

Particle, S – Secondary, B – Biogenic and Biomass Burning) into two sets: VBIS/PBIS (BI - Biogenic) for biogenic sources, and VBBS/PBBS (BB – Biomass Burning) for biomass burning sources.

Initial and boundary conditions were provided by MOZART (Model of Ozone and Related Chemical Tracers) global model data MOZART-4/GEOS-5 (Horowitz et al., 2003) with a time resolution of 6 hours. The ozone column densities were obtained from Total Ozone Mapping Spectrometer (TOMS) data by the National Aeronautics and Space Administration (ftp://toms.gsfc.nasa.gov/pub/omi/data/) and photolysis rates were calculated using the Tropospheric Ultraviolet and Visible (TUV) Radiation Model version 4.8 (NCAR, 2011). Anthropogenic emissions of non-methane volatile organic compounds (NMVOCs), SO_2, NO_x, CO, NH_3, PM_{10} and $PM_{2.5}$ were obtained from the high-resolution European emission inventory TNO-MACC (Monitoring Atmospheric Composition and Climate)-III. As an update to TNO-MACC-II (Kuenen et al., 2014), TNO-MACC-III has a major improvement in spatial distribution proxies, especially for urban areas (van Der Gon, 2015). The NMVOCs speciation was conducted following the approach described by Passant (2002). The PM emissions were further split into organic carbon, elemental carbon, sodium, sulphate and crustal minerals, based on country specific profiles provided by TNO.

2.2 Biogenic emission models

Two different biogenic emission models were used to calculate BVOCs emissions (isoprene, MT, SQT), i.e., MEGAN version 2.1 (Guenther et al., 2012) and the BVOC model developed by the Laboratory of Atmospheric Chemistry, Paul Scherrer Institute (Andreani-Aksoyoglu and Keller, 1995) (referred to as PSI model in this study). MEGAN is among the most widely used modelling systems estimating emission rates of BVOCs from terrestrial ecosystems. The MEGAN version 2.1 covers 147 individual BVOC species within 19 categories (Guenther et al., 2012). The PSI model was first developed for fine-resolution estimation of monoterpene and isoprene emissions in Switzerland (Andreani-Aksoyoglu and Keller, 1995) and was later expanded to the European domain (Oderbolz et al. (2013) Oikonomakis et al. (2018). Both the MEGAN and PSI model estimate biogenic emissions by an empirical bottom-up approach with similar algorithms based on standard emission rates (at leaf temperature of 30 ^oC and photosynthetically active radiation of 1000 µmol m^{-2} s^{-1}) and the emission response to environmental conditions (Guenther et al., 2012;Andreani-Aksoyoglu and Keller, 1995). The major difference between the two models is that MEGAN uses PFT (plant function type) specific emission factors, while the PSI model uses plant species specific emission factors. Here we mainly focus on the differences in the calculation of emission rates and inputs of land use and vegetation. A general comparison between the major inputs of the PSI model and MEGAN v2.1 is presented in Table 1.

2.2.1 Emission rates

MEGAN estimates the reference emission rates by emission factors of 15 PFTs as listed in Table 1. The Global Emission Factors (version 2011) from the MEGAN website (http://lar.wsu.edu/megan/guides.html) were used in this study. Emission factors of compounds are given for each of the 15 PFTs (Guenther et al., 2012). Tree species based emission factors and forest species composition profiles for more than 2000 ecoregions worldwide were used to generate the high resolution ($0.0083^o \times 0.0083^o$) global emission factor dataset. On the other hand, the PSI model uses reference emission rates of typical plant species in Europe (see Table 1). The reference emission rates (µg g(dry weight)$^{-1}$ h^{-1}) of isoprene and monoterpenes from forests, pasture and crops were

Atmos. Chem. Phys. Discuss., https://doi.org/10.5194/acp-2018-920
Manuscript under review for journal Atmos. Chem. Phys.
Discussion started: 17 October 2018
© Author(s) 2018. CC BY 4.0 License.

calculated based on algorithms given by Lamb et al. (1993). Isoprene emissions from Norway spruce were assumed to be about 10% of α-pinene emission rates during daytime (Keller et al., 1995). Sesquiterpenes (SQT) are the least studied among the identified BVOCs due to their high reactivity and relatively low vapor pressure (Duhl et al., 2008). Determination of their basal emission rates is therefore challenging (Niinemets et al., 2011). In the PSI model, SQT emissions were treated only as pool emissions and assumed to be 5% (by weight) of the monoterpene emissions based on field measurements from various studies (Steinbrecher et al., 2009).

2.2.2 Response functions

Isoprene, one of the most important BVOC species, is released after biosynthesis by volatilization, which depends on both temperature and solar radiation. On the other hand, monoterpenes are stored in large storage pools after their production in the plant organs. Emissions of monoterpenes are mostly temperature-dependent, although there are some species that have both light and temperature dependent synthesis emissions of MTs (Tingey et al., 1980). In the PSI model, the isoprene emissions are corrected by light (γ_L) and temperature (γ_T) response functions based on the algorithm described by Guenther et al. (1993):

$$\gamma_L = \frac{\alpha C_{L1} PAR}{\sqrt{1+\alpha^2 PAR^2}} \quad (1)$$

$$\gamma_T = \frac{\exp[C_{T1}(T-T_s)/RT_sT]}{1+\exp[C_{T2}(T-T_M)/RT_sT]} \quad (2)$$

where α (= 0.0027), C_{L1} (= 1.066), C_{T1} (= 95,000 J mol^{-1}), C_{T2} (= 230,000 J mol^{-1}), T_M (= 314 K) are all empirical coefficients determined by nonlinear fitting based on emission rate measurements, R is the gas constant (8.314 J K^{-1} mol^{-1}), and T_s is the standard leaf temperature (303.16 K). The response functions of the isoprene emission in MEGAN are based on Guenther et al. (1999), an updated version of Guenther et al. (1993). The major difference of the improved algorithm is the inclusion of the influence of past temperature and light conditions. New empirical coefficients T_{opt} and E_{opt} calculated by the average leaf temperature over the past 24 and 240 hours are added to include the continuous influence over time, respectively (Eq. 3):

$$\gamma_T = \frac{E_{opt} \times C_{T2} \times \exp(C_{T1} \times x)}{C_{T2} - C_{T1} \times (1-\exp(C_{T2} \times x))} \quad (3)$$

where, $x = [(1/T_{opt}) - (1/T)]/0.00831$. A detailed introduction to T_{opt} and E_{opt} can be found in Guenther et al. (2006).

For the light-independent response of MT pool emissions, similar exponential corrections are used by MEGAN and the PSI model which are based on Lamb et al. (1993) and Tingey et al. (1980) as shown in Eq. 4:

$$E = E_s \times \exp(\beta \times (T - Ts)) \quad (4)$$

where E is the MT emission at temperature T, E_s is the emission under standard conditions (T_s = 30 ^{o}C), and β is the slope coefficient of dlnE dT^{-1}. The slope value β has a wide range between 0.057 to 0.144 according to previous literature (Guenther et al., 1993). The value of 0.1 is used for MT in MEGAN2.1, while the values are between 0.065 to 0.077 for different MT species in the PSI model. The latter also includes light-dependent synthesis emissions of monoterpenes from Norway spruce based on the study of Schürmann (1993). In addition

© Author(s) 2018. CC BY 4.0 License.

to the light and temperature response, MEGAN v2.1 covers also some other factors such as leaf age, leaf area index, soil moisture, and CO_2 inhibition (Guenther et al., 2012).

The variation of light and temperature within the forest canopy are corrected by a canopy model in both the PSI model and MEGAN. The PSI model uses the canopy model by Baldocchi et al. (1985) combined with experiments in Hartheim Forest (Germany) and Central Switzerland (Joss, 1995). The detailed algorithm of the canopy correction for the PSI model was reported by Keller et al. (1995). The MEGAN canopy environmental model is based on Guenther et al. (1999), which estimates incident PAR and temperature of sun and shade leaves at different canopy depths. Details can be found in Guenther et al. (2006; 2012).

2.2.3 Inputs of driving variables

Three types of basic driving variables are required for both MEGAN and the PSI model, namely meteorological conditions, land use and biomass density. The meteorological data provide hourly, gridded information of temperature, solar radiation, humidity and surface pressure to drive the model simulation of emission response. We used the same meteorological data retrieved from the WRF-ARW model as input for both models. The main difference between the two model inputs is in the land use and leaf biomass density.

MEGAN v2.1 uses the Community Land Model version 4 (CLM4) including 15 PFTs as shown in Table 1. In this study, we adopted for MEGAN the same global PFT map as in Sindelarova et al. (2014) with a resolution of 0.05 degrees. For the PSI model, the GlobCover 2006 inventory by European Space Agency (http://due.esrin.esa.int/page_globcover.php) was used. This inventory was developed based on MERIS (MEdium Resolution Imaging Spectrometer) FRS (Fine Resolution Full Swath product) level 1B data during December 2004 to June 2006 (Bicheron et al., 2008). The raw data has a fine resolution of 300 m and 64 categories of land use types. The grid-scale fractions of needleleaf, broadleaf and mixed forests were first calculated based on the GlobCover inventory data. The mixed forest was assumed to be composed of 50% needleleaf and 50% broadleaf species. Different tree species in the same category may have different emission factors. For instance, although all belong to broadleaf tree species, oak (*Quercus*) has high emission rate, while beech (*Fagus sylvatica*) and maple (*Acer*) are negligible BVOC emitters. Even within the same genus, there might be large differences in emissions, e.g. two oak species, where quercus robur is a high isoprene emitter and quercus suber a low isoprene emitter (Steinbrecher et al., 2009). Therefore, in the PSI model, we split the forests into 10 typical forest species (see Table 1) found in Europe based on the country-specific forest species profile from Simpson et al. (1999).

The variation of biomass density in MEGAN was simulated by the satellite data of the leaf area index (LAI, m^2 leaves per m^2 projected area) with a time step of 8 days. The TERRA/MODIS vegetation data products MOD15A2 were downloaded from the NASA Earth Observations website (https://neo.sci.gsfc.nasa.gov/view.php?datasetId=MOD15A2_E_LAI). The grid-scale LAI was then divided by the fraction of vegetation coverage of each grid (sum of PFT) to get the average LAI of vegetation covered surfaces (LAIv).

As the reference emission rates of the PSI model are based on dry weight of leaf biomass, the leaf biomass density factors (g dry weight per m^2 projected area) of each tree species (Cannell, 1982; Satoo and Madgwick, 1982) were explicitly used in the PSI model. To simulate the vertical variation of foliar biomass in the canopy, the biomass density was scaled by the leaf area distribution in each canopy layer as described in Oderbolz et al. (2013). The temporal variation of the biomass was simulated by monthly factors for different plant types. For

© Author(s) 2018. CC BY 4.0 License.

example, the PSI model assumes that the leaf biomass of deciduous trees, such as oak and larch, turn to zero in the winter months (November - March) and crops only have biomass in the growing season (April - August).

2.3 Observation datasets and statistics

Two types of measurement datasets were used to evaluate the model results. Measurements of hourly ozone concentrations in 2011 were extracted from the European air quality database AirBase v7 by the European Environment Agency (Mol and Leeuw, 2005). To reduce the uncertainties arising from the model resolution, only ozone measurements at background-rural stations were used in the model evaluation. Concentrations of OA and secondary inorganic aerosol (particulate nitrate, sulphate, and ammonium) were obtained from ACSM/ AMS measurements at 8 stations: Zurich (Canonaco et al., 2013), Mace Head (Ovadnevaite et al., 2014; Schmale et al., 2017), Montsec (Ripoll et al., 2015), Bologna and San Pietro Capofiume (Gilardoni et al., 2014), Paris SIRTA (Site Instrumental de Recherche par Télédétection Atmosphérique) (Petit et al., 2015), Marseille (Bozzetti et al., 2017), and Finokalia (as continuation of Hildebrandt et al. (2010)). The spatial distribution of the measurement sites is shown in Fig. 1. Zurich, Bologna and Marseille are urban sites, Paris SIRTA is a suburban site, while Mace Head, Finokalia, San Pietro Capofiume and Montsec are in rural or remote areas. We divided the whole domain into 3 regions to enable a comparison for different latitudes: northern Europe (NE, 55^{o}N – 70^{o}N), central Europe (CE, 45^{o}N – 55^{o}N) and southern Europe (SE, 35^{o}N – 45^{o}N). The time span of OA observations at each station is shown in Fig. S1. The measurements cover nearly the whole year of 2011 in Zurich (except for January) and Mace Head (except for November and December), while other stations cover shorter periods (Fig. S1). The modelled concentrations at the surface (1^{st}) layer were interpolated to the location of the stations to compare with the measurements. The statistical metrics, such as mean bias (MB), mean error (ME), mean fractional bias (MFB), mean fractional error (MFE) and root mean square error (RMSE), were calculated and compared for two CAMx simulations using different BVOC emissions obtained by MEGAN and the PSI model. The definitions of these statistical metrics are presented in Table S1.

3 Results and discussion

3.1 Biogenic VOC emissions in Europe

BVOC emissions estimated by the PSI model and MEGAN showed significant differences in both spatial and temporal variations. To demonstrate the seasonal differences, we compared the BVOC emissions in February and July to represent winter and summer periods, respectively. BVOC emissions in winter are much lower than in summer, especially for isoprene which is mainly emitted by deciduous broadleaf trees. The PSI model produced negligible isoprene in winter, as the leaf biomass of oak trees, the largest isoprene emitters, was set to zero during that period. For monoterpenes, which are mainly emitted by evergreen needleleaf forests, the seasonal difference was less obvious than for isoprene, although the emissions in winter were lower than in summer due to lower temperatures (about 82% and 96% lower than in summer for the PSI model and for MEGAN, respectively).

Isoprene emissions by MEGAN were substantially higher than those in the PSI model (Fig. 2a) by a factor of 2.9 on average in summer. The highest difference occurred in Southern Europe (Fig. S2a), where the highest grid-scale absolute difference (MEGAN – PSI) reached 203 kg $cell^{-1}$ h^{-1} in Spain. The major reason for

© Author(s) 2018. CC BY 4.0 License.

low isoprene emissions by the PSI model is the assumption of oak being the main broadleaf tree species emitting isoprene, while all the broadleaf trees and shrubs (PFT4 - PFT11) have positive emission factors in MEGAN. On the other hand, the PSI model estimated in general more monoterpene emissions than MEGAN (Fig. 2b). The total emissions in the whole domain were 486 t h^{-1} (winter) and 2768 t h^{-1} (summer) for the PSI model, while the values were only 40 t h^{-1} (winter) and 994 t h^{-1} (summer) for MEGAN. Accordingly, the average MT emissions in the PSI model were higher than MEGAN by a factor of 12.2 and 2.8 in winter and summer, respectively. Significantly higher MT emissions by the PSI model can be observed in Scandinavia, the Iberian Peninsula and southeast Europe (Fig. S2b). The only areas where the PSI model estimated lower MT emissions than MEGAN were in Italy, the Balkans and France, due to a relatively lower needleleaf forest coverage in these regions (Fig. S3). The difference in SQT emissions by two models was smaller in magnitude (average SQT-PSI is 4.1% higher than SQT-MEGAN in summer) compared with other BVOCs species with a similar pattern of spatial difference as for MT. (Fig 2c, Fig S2c).

The diurnal variations of the isoprene and monoterpene emissions showed a peak around noon for both models (Fig. 3). In winter, highest isoprene emissions occurred in Central Europe (CE) for PSI model, while in Southern Europe (SE) for MEGAN. The main reason is isoprene-PSI mainly came from Norway Spruce in the CE instead of deciduous trees in the south during winter time. Although the shapes of the curves were quite similar, MEGAN showed steeper changes ([emission(t) - emission(t-1)] / emission(t)) due to larger slope coefficient β value used in the exponential temperature response function. Especially for monoterpenes in southern Europe (SE) in summer, the highest increase and decrease rates reached 43.8% (at UTC 05:00) and -57.1% (at UTC 18:00), respectively, while in the PSI model the hourly changes varied between 18.6% (at UTC 9:00) and -15.6% (at UTC 19:00).

These results agree well with previous inter-comparison studies. Comparisons between models and observations suggested that MEGAN tends to overestimate isoprene emissions (Bash et al., 2016; Carlton and Baker, 2011), and to underpredict monoterpene emissions (Emmerson et al., 2016; Poupkou et al., 2010; Silibello et al., 2017). However, due to limited measurement data and large uncertainties, it is not possible to conclude which model predicts more reliable BVOC emissions. An uncertainty of a factor of up to 5 for estimates of isoprene and monoterpene emissions was reported in Europe (Simpson et al., 1999). In the current study, the domain average emissions differed by a factor of 0.3 for isoprene and 2.8 for MT (PSI / MEGAN) in summer.

3.2 Influence of different BVOC emissions on the modelling of ozone and aerosols

3.2.1 Ozone

The modelled ozone mixing ratios from two simulations using the biogenic emissions calculated by the PSI model (O_3-PSI) and MEGAN (O_3-MEGAN) were evaluated by the measurements from the European air quality database AirBase (Mol and Leeuw, 2005). Table 2 shows the statistical metrics of modelled average mixing ratios of afternoon (12:00–18:00 UTC) surface ozone at 537 rural background stations. The model performance in summer was generally better than in winter for all regions, but the difference between the PSI model and MEGAN was small. In winter, the two models showed similar mean bias (~3 ppb) and RMSE (~9.2 ppb) between modelled and measured concentration. In summer, the PSI model showed lower (34.0%) mean bias but slightly higher (1.3%) RMSE than MEGAN. To investigate the difference in more detail, we compared the bias

© Author(s) 2018. CC BY 4.0 License.

between modelled and observed O_3 in different mixing ratio bins for different regions in summer (Fig. 4). In general, ozone modelled using the BVOC emission input from both models was overestimated at low mixing ratios and underestimated at high mixing ratios. A similar pattern was found in previous O_3 modelling studies in Europe (Im et al., 2015; Oikonomakis et al., 2018; Solazzo et al., 2017). CAMx performed better with MEGAN emissions at most stations at the high ozone bins. Although the PSI model led to lower overall MB (Table 2), it was mostly due to compensation at the low and high O_3 level bins.

To further explore the reasons for the different model performance in the ozone simulations, we present the spatial distributions of modelled ozone in summer calculated using BVOC emissions from the PSI model and MEGAN in Fig. 5. O_3-PSI was generally lower than O_3-MEGAN in whole Europe. In summer, the largest effect of using different BVOC emissions on ozone was mostly in southern Europe, especially in the Mediterranean region, with the highest relative difference between O_3-PSI and O_3-MEGAN reaching -14% (7.5ppb, in Italy); while in UK and Ireland, where isoprene emissions by PSI model were higher than MEGAN (Fig. S2), a positive difference up to 3.9 ppb was observed. A positive correlation was observed between the spatial difference in simulated O_3 and isoprene emissions. As an important ozone precursor, isoprene reacts with hydroxyl radicals (OH) to form peroxyl radicals (RO_2, HO_2) which further react with NO to generate NO_2 and finally ozone (Wennberg et al., 2018). This process can be significantly affected by the availability of isoprene and NO_x in the atmosphere as well as temperature (Calfapietra et al., 2013), leading to high uncertainties in the net influence of BVOC emissions. Li et al. (2007) found that increasing the isoprene emissions by 50% resulted in an increase of the O_3 mixing ratios by 5 –25 ppb in urban Houston in the United States, and Zare et al. (2012) suggested that the 21% higher annual isoprene emissions by MEGAN than GEIA (Global Emissions Inventory Activity) led to up to 10% higher O_3 concentrations in the African Savannah. However, the effect of the BVOC emissions on the ozone levels in Europe was much smaller in this study. The about 3 times higher isoprene emissions in MEGAN led only to up to ~10% (7 ppb) higher ozone mixing ratios in summer compared to the PSI model. Similarly, an earlier study by Aksoyoglu et al. (2012) using the PSI model for BVOC emissions suggested that increasing the isoprene emissions by a factor of four in Europe led to an increase of less than 10% in the afternoon ozone mixing ratios. The main reason for the weak effect of isoprene on ozone could be that ozone formation in Europe is mostly sensitive to NO_x emissions rather than VOC emissions, as well as rather low ozone production compared with background (Oikonomakis et al., 2018; Sartelet et al., 2012).

3.2.2 Organic aerosols

The effects of different BVOC emissions on organic aerosols were investigated by comparing modelled OA concentrations with measurements at 8 ACSM/AMS stations. Although the OA concentrations were generally underpredicted in both cases, the model performance for OA was better with the PSI biogenic emissions (Fig. 6). About 67% of the modelled OA concentrations were below the 1:2 line in the case of MEGAN (Fig. 6b). The mean bias between observed and modelled OA concentrations with the PSI BVOC emissions was lower than the bias obtained with MEGAN emissions (3.9% in Paris – 83.4% in Mace Head, see Table 3). The better model performance when using the PSI emissions was more obvious at rural or remote stations where biogenic sources play a major role in OA formation. The mean bias of OA by the PSI model was 21 % to 83% lower than MEGAN at rural or remote stations (Finokalia, San Pietro Capofiume, Montsec and Mace Head), while the range was 4% - 12% for Paris, Bologna and Marseille (see Table 3). The situation of Zurich was different with

© Author(s) 2018. CC BY 4.0 License.

an MB reduction of 67% by PSI model compared with MEGAN as an urban station, mostly because the station is an urban background site that is strongly affected by biogenic emissions (Daellenbach et al., 2017).

We further evaluated the model performance of the temporal variation at Zurich and Mace Head as examples of urban background and rural stations, respectively (Fig. 7, top panels), because these two datasets covered almost the whole year. In spite of some underestimation, the temporal variation was well captured. At Zurich, the difference between the two cases (OA-PSI and OA-MEGAN) was small in February and March and they were both lower than the measurements, possibly due to underestimation of biomass burning OA (Fountoukis et al., 2014). The largest difference occurred in the fall when OA-PSI reproduced the measurements quite well, while OA-MEGAN showed a large underestimation. This is consistent with source apportionment studies performed for Zurich (Canonaco et al., 2013; Canonaco et al., In prep.; Daellenbach et al., 2017), which reported that the contribution of biogenic sources to OA was minor in the period of January to March and significant (>50%) in summer and fall.

The situation was quite different for Mace Head. Located on the west coast of Ireland and 90 km away from the closest city Galway (Schmale et al., 2017), Mace Head is a remote station with low influence from the anthropogenic activities (O'Dowd et al., 2014). The simulation with the PSI biogenic emission model could reproduce all the measured peaks quite well, while the simulation using the MEGAN emissions failed to capture their magnitude. To investigate the cause of the high OA concentrations during certain periods, 72-hour back trajectory analyses ending at Mace Head on 26 March (as an example for a high-OA day) and on 4 August (as an example for a low-OA day) were conducted by NOAA's HYSPLIT atmospheric transport and dispersion modelling system (Stein et al., 2015). According to the HYSPLIT results (Fig. S4), the air masses were transported from Ireland and Scotland during the high-OA period (Fig. S4a), while during the low-OA period the air masses came from the North Atlantic Ocean (Fig. S4b), suggesting that the OA peaks originated from anthropogenic or biogenic sources on land. The influence of wind direction was further studied by comparing modelled and measured OA during the two periods featured by land-wind (24-26 March) and marine-wind (2-4 August) in Fig. S5. Measured OA in period with dominant wind direction from land was higher than during the marine-wind dominant periods by a factor of ~10. Modelled OA-PSI was very close to measurements while OA-MEGAN was underestimated in both periods. However, it is not possible to conclude that the good model performance for OA with PSI emissions is due to the fact that its high MT emissions are more accurate. It could also be due to the overestimated MT emissions compensating other missing continental sources of OA, e.g. biomass burning.

The spatial distribution of the SOA difference showed a similar pattern as its main precursor, monoterpenes (Fig. 8). The PSI emissions lead to significantly higher (by 113% and 109% in winter and summer, respectively) SOA production than MEGAN. The grid-scale difference reached up to a factor of 35 and 17 for winter and summer SOA, respectively. The largest differences occurred in central Europe, the Iberian Peninsula and Turkey in winter, and especially in Scandinavia in summer.

The modelled POA was also slightly higher (6.5% in winter and 7.8% in summer for average) with PSI emissions compared to the case with MEGAN (Fig. S6). Unlike in the traditional CTMs, where POA is treated as inert, the VBS scheme of CAMx allows POA to evaporate and react with oxidants. According to the partitioning theory (Donahue et al., 2006; Odum et al., 1996), higher total OA concentrations lead to higher partitioning to the particle phase for all compounds that are soluble in the aerosol matrix. Therefore, in our case,

© Author(s) 2018. CC BY 4.0 License.

the high OA-PSI shifted the particle – gas equilibrium of primary condensable gases towards the particle phase, resulting in higher POA.

3.2.3 Inorganic aerosols

The influence of BVOC emissions on secondary inorganic aerosols (SIA) was much smaller than on SOA according to the comparison of model results with measurements (Table 3). At the eight ACSM/AMS stations, using the PSI emissions generally reduced the RMSE between modelled and measured particulate nitrate (PNO_3), sulphate (PSO_4), and ammonium (PNH_4) by up to 15.0%, 1.7%, and 7.7%, respectively, compared to CAMx simulations with the MEGAN emissions. Only Finokalia (Greece, rural) and San Pietro Capofiume (Italy, rural) had lower RMSE with the MEGAN emissions. Unlike the obvious difference in OA, difference between the modelled temporal variations of the inorganic aerosol was negligible with the two emission estimates (Fig. 7). The PNO_3-MEGAN was slightly higher than PSI, because lower MT emission by MEGAN lead to lower MT-NO_3 reaction and therefore more NO_x were available to be oxidized to PNO_3 (Fig. S8).

The modelled and measured daily average concentrations match well except for February and March at Zurich, when temperature was significantly underestimated and resulted in higher condensation (Fig. S7a). A similar effect of temperature was not observed in OA during the same period, possibly due to compensation of underestimated winter OA as a consequence of lacking sources in the model, especially biomass burning (Ciarelli et al., 2017). On the other hand, the modelled primary elemental carbon (PEC) matched the measurements at Zurich very well.

Similar to the situation of OA, the measured SIA (PSO_4, PNO_3 and PNH_4) at Mace Head peaked during the periods with wind from land. Both biogenic models captured the peaks well but overestimated the SIA during the peak periods. The modelled elemental carbon concentrations (PEC, in Fig. 7) on the other hand, were lower than the measured equivalent black carbon (EBC) in general but followed the temporal variation very well. In a study about the aerosols at Mace Head, O'Dowd et al. (2014) reported that EBC measurements can significantly overestimate black carbon concentration by up to 50% or more. Overestimation of SIA could result from either too high precursor emissions or too much particle formation in the aqueous phase. The precursor gases SO_2 and NO_x from anthropogenic sources (continental, shipping) (Fig. S8) might be accumulated too much in the surface layer (due to lack of vertical distribution of elevated emissions) leading to too high SIA formation.

The differences in the spatial distributions of PSO_4, PNO_3 and PNH_4 between the two simulations with PSI and MEGAN emissions are shown in Fig. 9. The inorganic aerosol concentrations varied by less than 15% on the grid scale for the different BVOC emissions. Highest PSO_4 levels were predicted in central and eastern Europe in winter, where SO_2 emissions are higher, while in summer the elevated sulphate concentrations were mostly along the shipping routes (Fig. 9). The PSI BVOC emissions lead to higher PSO_4 than MEGAN, especially over the area from southern Poland to Turkey through the Balkan Peninsula in summer. These regions have the highest SO_2 emissions in the model domain due to large combustion based power plants and coal burning. In summer, the main pathway for sulphate formation in southern Europe is the gas-phase oxidation of SO_2 with OH radical (Chrit et al., 2018; Megaritis et al., 2013). The higher sulphate concentrations predicted by CAMx with PSI BVOC emissions are consistent with the spatial pattern of the differences between PSI-MEGAN simulations for SO_2 concentrations and OH radicals (Fig. S9) due to the following: As reaction with

© Author(s) 2018. CC BY 4.0 License.

OH radical is the largest loss pathway for isoprene in the atmosphere (Wennberg et al., 2018), higher isoprene emissions in MEGAN consumes more OH radical. As a consequence, less SO_2 is oxidized to form PSO_4 when MEGAN emissions are used (Fig. S9), leading to lower PSO_4 formation.

Formation of PNO_3 depends on the availability of NO_x and NH_3 emissions (Aksoyoglu et al., 2011; Wen et al., 2015). In contrast to PSO_4, PNO_3 and PNH_4 concentrations modelled using the PSI biogenic emissions were generally lower than those using MEGAN emissions, especially in regions where PSI model has more MT emissions (Fig. S2b). Nitrate radicals are recognized as a significant sink for BVOCs, especially monoterpenes at night (while OH oxidation is more relevant for isoprene during daytime) (Kiendler-Scharr et al., 2016; Ng et al., 2017). Higher monoterpene emissions produced by the PSI model lead to larger consumption of nitrate radicals affecting PNO_3 formation from HNO_3 and NH_3. These results are consistent with a recent study showing the significant effect of BVOCs on ammonium nitrate (Aksoyoglu et al., 2017).

4 Conclusions

In this study, the European air quality in the year 2011 was simulated by the regional air quality model CAMx using two biogenic volatile organic compound (BVOC) emission models: MEGAN and PSI model. The model results were evaluated by O_3 measurements from the European air quality database AirBase v7 as well as the aerosol measurements at 8 ACSM/AMS stations. The results indicate that MEGAN generates more isoprene (by a factor of about 3), but less (~36%) monoterpene emissions than the PSI model in Europe in summer, mainly due to their different vegetation classification and reference emission rates. In spite of much higher isoprene emissions, simulations with MEGAN led to only slightly higher (7 ppb, <10%) ozone concentrations in summer compared to PSI emissions, especially in southern Europe. The evaluation of model results showed that PSI emissions improve the model performance for low ozone mixing ratios, but they worsen it at mixing ratios above 60 ppb.

The largest effect of using different BVOC emissions was predicted to be on SOA. PSI emissions led to higher SOA concentrations by about 110% compared to MEGAN due to higher monoterpene emissions, and therefore show a better model performance for OA at all 8 measurement sites. A more detailed evaluation of modelled organic and inorganic aerosols was performed at Zurich and Mace Head where aerosol measurements were available for relatively longer periods. Comparison of modelled and measured OA at Zurich suggested that OA concentrations could be captured very well with PSI BVOC emissions most of the time except in winter when modelled OA was underestimated by both PSI and MEGAN emissions. These results pointed out the missing winter sources such as biomass burning. On the other hand, at the remote site Mace Head, aerosol concentrations were affected by the prevailing air masses. Using PSI biogenic emissions, we could reproduce the OA peaks almost perfectly while OA concentrations were significantly underestimated when MEGAN biogenic emissions were used. One should however keep in mind that good model performance could also be due to compensation of other factors.

Effects of using different BVOC emission models on secondary inorganic aerosols (particulate nitrate, sulphate, ammonium) were relatively small (< 15%). The mean bias between modeled and measured values was lower when PSI model was used. The results of this study emphasize the importance of BVOC emissions in ozone and organic aerosol simulations and model intercomparison studies. In future studies, BVOC emission

© Author(s) 2018. CC BY 4.0 License.

models with more regional specific adaptation in vegetation types and emission factors are urgently needed to reduce the uncertainties in BVOC emission estimates in order to improve air quality modelling.

Data availability. The data of this study are available upon request from the corresponding authors.

Acknowledgements. We would like to thank the TNO for providing anthropogenic emissions, European Centre for Medium-Range Weather Forecasts (ECMWF) for the access to the meteorological data, the European Environmental Agency (EEA) for the air quality data, the National Aeronautics and Space Administration (NASA) and its data-contributing agencies (NCAR, UCAR) for the TOMS and MODIS data, the global air quality model data and the TUV model. Simulation of WRF and CAMx models were performed at the Swiss National Supercomputing Centre (CSCS). We are grateful to RAMBOLL for the valuable support for CAMx. We thank the ACSM/AMS data providers, namely Stefania Gilardoni for Bologna and San Pietro Capofiume stations; Nicolas Marchand and MASSALYA Instrumental Plateform (https://lce.univ-amu.fr/en/massalya) for Marseille; Olivier Favez (INERIS) and the whole SIRTA team for measurements conducted in the Paris area in the frame of the EU FP7 ACTRIS program under the grant agreement n° 262254; Kalliopi Florou for Finokalia. EPA-Ireland (AEROSOURCE, 2016-CCRP-MS-31) is acknowledged, as well as EGAR group from IDAEA-CSIC (special mention to Anna Ripoll and Andrés Alastuey) and Generalitat de Catalunya (AGAUR 2017 SGR41). M.C. Minguillón acknowledges the Ramón y Cajal fellowship awarded by the Spanish Ministry of Economy, Industry and Competitiveness.

References

Aksoyoglu, S., Keller, J., Barmpadimos, I., Oderbolz, D., Lanz, V. A., Prévôt, A. S. H., and Baltensperger, U.: Aerosol modelling in Europe with a focus on Switzerland during summer and winter episodes, Atmos. Chem. Phy., 11, 7355-7373, 10.5194/acp-11-7355-2011, 2011.

Aksoyoglu, S., Keller, J., Oderbolz, D. C., Barmpadimos, I., Prévôt, A. S. H., and Baltensperger, U.: Sensitivity of ozone and aerosols to precursor emissions in Europe, Int. J. Environ. Pollut., 50, 451-459, 10.1504/ijep.2012.051215, 2012.

Aksoyoglu, S., Ciarelli, G., El-Haddad, I., Baltensperger, U., and Prévôt, A. S. H.: Secondary inorganic aerosols in Europe: sources and the significant influence of biogenic VOC emissions, especially on ammonium nitrate, Atmos. Chem. Phy., 17, 7757-7773, 10.5194/acp-17-7757-2017, 2017.

Andreani-Aksoyoglu, S., and Keller, J.: Estimates of monoterpene and isoprene emissions from the forests in switzerland, J. Atmos. Chem, 20, 71-87, 10.1007/bf01099919, 1995.

Ayres, B. R., Allen, H. M., Draper, D. C., Brown, S. S., Wild, R. J., Jimenez, J. L., Day, D. A., Campuzano-Jost, P., Hu, W., de Gouw, J., Koss, A., Cohen, R. C., Duffey, K. C., Romer, P., Baumann, K., Edgerton, E., Takahama, S., Thornton, J. A., Lee, B. H., Lopez-Hilfiker, F. D., Mohr, C., Wennberg, P. O., Nguyen, T. B., Teng, A., Goldstein, A. H., Olson, K., and Fry, J. L.: Organic nitrate aerosol formation via NO3 + biogenic volatile organic compounds in the southeastern United States, Atmos. Chem. Phy., 15, 13377-13392, 10.5194/acp-15-13377-2015, 2015.

Baldocchi, D. D., Hutchison, B. A., Matt, D. R., and McMillen, R. T.: Canopy radiative-transfer models for spherical and known leaf inclination angle distributions - a test in an oak hickory forest, J. App. Eco., 22, 539-555, 10.2307/2403184, 1985.

Bash, J. O., Baker, K. R., and Beaver, M. R.: Evaluation of improved land use and canopy representation in BEIS v3.61 with biogenic VOC measurements in California, Geosci. Model Dev., 9, 2191-2207, 10.5194/gmd-9-2191-2016, 2016.

Bessagnet, B., Pirovano, G., Mircea, M., Cuvelier, C., Aulinger, A., Calori, G., Ciarelli, G., Manders, A., Stern, R., Tsyro, S., Vivanco, M. G., Thunis, P., Pay, M. T., Colette, A., Couvidat, F., Meleux, F., Rouil, L., Ung, A., Aksoyoglu, S., Baldasano, J. M., Bieser, J., Briganti, G., Cappelletti, A., D'Isidoro, M., Finardi, S., Kranenburg, R., Silibello, C., Carnevale, C., Aas, W., Dupont, J. C., Fagerli, H., Gonzalez, L., Menut, L., Prévôt, A. S. H., Roberts, P., and White, L.: Presentation of the EURODELTA III intercomparison

© Author(s) 2018. CC BY 4.0 License.

exercise - evaluation of the chemistry transport models' performance on criteria pollutants and joint analysis with meteorology, Atmos. Chem. Phy., 16, 12667-12701, 10.5194/acp-16-12667-2016, 2016.

Bicheron, P., Defourny, P., Brockmann, C., Schouten, L., Vancutsem, C., Huc, M., Bontemps, S., Leroy, M., Achard, F., Herold, M., Ranera, F., and Arino, O.: GLOBCOVER: Products Description and Validation Report, Medias France, Toulouse Cedex, France, 2008.

Bonn, B., von Kuhlmann, R., and Lawrence, M. G.: High contribution of biogenic hydroperoxides to secondary organic aerosol formation, Geophys. Res. Lett., 31, 10.1029/2003gl019172, 2004.

Bozzetti, C., El Haddad, I., Salameh, D., Daellenbach, K. R., Fermo, P., Gonzalez, R., Minguillon, M. C., Iinuma, Y., Poulain, L., Elser, M., Muller, E., Slowik, J. G., Jaffrezo, J. L., Baltensperger, U., Marchand, N., and Prévôt, A. S. H.: Organic aerosol source apportionment by offline-AMS over a full year in Marseille, Atmos. Chem. Phy., 17, 8247-8268, 10.5194/acp-17-8247-2017, 2017.

Calfapietra, C., Fares, S., Manes, F., Morani, A., Sgrigna, G., and Loreto, F.: Role of Biogenic Volatile Organic Compounds (BVOC) emitted by urban trees on ozone concentration in cities: A review, Environ. Pollut., 183, 71-80, 10.1016/j.envpol.2013.03.012, 2013.

Cannell, M. G. R.: World forest biomass and primary production data, Academic Press, London, 1982.

Canonaco, F., Crippa, M., Slowik, J. G., Baltensperger, U., and Prévôt, A. S. H.: SoFi, an IGOR-based interface for the efficient use of the generalized multilinear engine (ME-2) for the source apportionment: ME-2 application to aerosol mass spectrometer data, Atmos. Meas. Tech., 6, 3649-3661, 10.5194/amt-6-3649-2013, 2013.

Canonaco, F., Slowik, J. G., Y., S., K., D., C., B., El-Haddad, I., Crippa, M., Huang, R.-J., Baltensperger, U., and Prévôt, A. S. H.: Source Finder Professional (SoFi Pro) allowing for time-dependent factor profiles and uncertainty assessment: application to one year of organic aerosol data, Atmos. Meas. Tech. Discuss., In prep.

Carlton, A. G., Pinder, R. W., Bhave, P. V., and Pouliot, G. A.: To What Extent Can Biogenic SOA be Controlled?, Environ. Sci. Technol., 44, 3376-3380, 10.1021/es903506b, 2010.

Carlton, A. G., and Baker, K. R.: Photochemical Modeling of the Ozark Isoprene Volcano: MEGAN, BEIS, and Their Impacts on Air Quality Predictions, Environ. Sci. Technol., 45, 4438-4445, 10.1021/es200050x, 2011.

Chang, J. S., Brost, R. A., Isaksen, I. S. A., Madronich, S., Middleton, P., Stockwell, W. R., and Walcek, C. J.: A 3-dimensional eulerian acid deposition model - physical concepts and formulation, J. Geophys. Res.-Atmos, 92, 14681-14700, 10.1029/JD092iD12p14681, 1987.

Chrit, M., Sartelet, K., Sciare, J., Pey, J., Nicolas, J. B., Marchand, N., Freney, E., Sellegri, K., Beekmann, M., and Dulac, F.: Aerosol sources in the western Mediterranean during summertime: a model-based approach, Atmos. Chem. Phys., 18, 9631-9659, 10.5194/acp-18-9631-2018, 2018.

Ciarelli, G., Aksoyoglu, S., El Haddad, I., Bruns, E. A., Crippa, M., Poulain, L., Äijälä, M., Carbone, S., Freney, E., O'Dowd, C., Baltensperger, U., and Prévôt, A. S. H.: Modelling winter organic aerosol at the European scale with CAMx: evaluation and source apportionment with a VBS parameterization based on novel wood burning smog chamber experiments, Atmos. Chem. Phy., 17, 7653-7669, 10.5194/acp-17-7653-2017, 2017.

Colette, A., Andersson, C., Manders, A., Mar, K., Mircea, M., Pay, M. T., Raffort, V., Tsyro, S., Cuvelier, C., Adani, M., Bessagnet, B., Bergström, R., Briganti, G., Butler, T., Cappelletti, A., Couvidat, F., D'Isidoro, M., Doumbia, T., Fagerli, H., Granier, C., Heyes, C., Klimont, Z., Ojha, N., Otero, N., Schaap, M., Sindelarova, K., Stegehuis, A. I., Roustan, Y., Vautard, R., van Meijgaard, E., Vivanco, M. G., and Wind, P.: EURODELTA-Trends, a multi-model experiment of air quality hindcast in Europe over 1990–2010, Geosci. Model Dev., 10, 3255-3276, 10.5194/gmd-10-3255-2017, 2017.

Curci, G., Beekmann, M., Vautard, R., Smiatek, G., Steinbrecher, R., Theloke, J., and Friedrich, R.: Modelling study of the impact of isoprene and terpene biogenic emissions on European ozone levels, Atmos. Environ., 43, 1444-1455, 10.1016/j.atmosenv.2008.02.070, 2009.

Daellenbach, K. R., Stefenelli, G., Bozzetti, C., Vlachou, A., Fermo, P., Gonzalez, R., Piazzalunga, A., Colombi, C., Canonaco, F., Hueglin, C., Kasper-Giebl, A., Jaffrezo, J. L., Bianchi, F., Slowik, J. G., Baltensperger, U., El-Haddad, I., and Prévôt, A. S. H.: Long-term chemical analysis and organic aerosol source apportionment at nine sites in central Europe: source identification and uncertainty assessment, Atmos. Chem. Phy., 17, 13265-13282, 10.5194/acp-17-13265-2017, 2017.

Dee, D. P., Uppala, S. M., Simmons, A. J., Berrisford, P., Poli, P., Kobayashi, S., Andrae, U., Balmaseda, M. A., Balsamo, G., Bauer, P., Bechtold, P., Beljaars, A. C. M., van de Berg, L., Bidlot, J., Bormann, N., Delsol, C., Dragani, R., Fuentes, M., Geer, A. J., Haimberger, L., Healy, S. B., Hersbach, H., Holm, E. V., Isaksen, L., Kallberg, P., Kohler, M., Matricardi, M., McNally, A. P., Monge-Sanz, B. M., Morcrette, J. J., Park, B. K., Peubey, C., de Rosnay, P., Tavolato, C., Thepaut, J. N., and Vitart, F.: The ERA-Interim reanalysis: configuration and performance of the data assimilation system, Q. J. Roy. Meteor. Soc., 137, 553-597, 10.1002/qj.828, 2011.

© Author(s) 2018. CC BY 4.0 License.

Donahue, N. M., Robinson, A. L., Stanier, C. O., and Pandis, S. N.: Coupled Partitioning, Dilution, and Chemical Aging of Semivolatile Organics, Environ. Sci. Technol., 40, 2635-2643, 10.1021/es052297c, 2006.

Emmerson, K. M., Galbally, I. E., Guenther, A. B., Paton-Walsh, C., Guerette, E. A., Cope, M. E., Keywood, M. D., Lawson, S. J., Molloy, S. B., Dunne, E., Thatcher, M., Karl, T., and Maleknia, S. D.: Current estimates of biogenic emissions from eucalypts uncertain for southeast Australia, Atmos. Chem. Phy., 16, 6997-7011, 10.5194/acp-16-6997-2016, 2016.

Fountoukis, C., Megaritis, A. G., Skyllakou, K., Charalampidis, P. E., Pilinis, C., Denier van der Gon, H. A. C., Crippa, M., Canonaco, F., Mohr, C., Prévôt, A. S. H., Allan, J. D., Poulain, L., Petäjä, T., Tiitta, P., Carbone, S., Kiendler-Scharr, A., Nemitz, E., O'Dowd, C., Swietlicki, E., and Pandis, S. N.: Organic aerosol concentration and composition over Europe: insights from comparison of regional model predictions with aerosol mass spectrometer factor analysis, Atmos. Chem. Phy., 14, 9061-9076, 10.5194/acp-14-9061-2014, 2014.

Fu, P. Q., Kawamura, K., Chen, J., and Miyazaki, Y.: Secondary Production of Organic Aerosols from Biogenic VOCs over Mt. Fuji, Japan, Environ. Sci. Technol., 48, 8491-8497, 10.1021/es500794d, 2014.

Gilardoni, S., Massoli, P., Giulianelli, L., Rinaldi, M., Paglione, M., Pollini, F., Lanconelli, C., Poluzzi, V., Carbone, S., Hillamo, R., Russell, L. M., Facchini, M. C., and Fuzzi, S.: Fog scavenging of organic and inorganic aerosol in the Po Valley, Atmos. Chem. Phy., 14, 6967-6981, 10.5194/acp-14-6967-2014, 2014.

Griffin, R. J., Cocker, D. R., Seinfeld, J. H., and Dabdub, D.: Estimate of global atmospheric organic aerosol from oxidation of biogenic hydrocarbons, Geophys. Res. Lett., 26, 2721-2724, 10.1029/1999gl900476, 1999.

Grote, R., and Niinemets, U.: Modeling volatile isoprenoid emissions - a story with split ends, Plant Biology, 10, 8-28, 10.1055/s-2007-964975, 2008.

Guenther, A., Baugh, B., Brasseur, G., Greenberg, J., Harley, P., Klinger, L., Serca, D., and Vierling, L.: Isoprene emission estimates and uncertainties for the Central African EXPRESSO study domain, J. Geophys. Res.-Atmos, 104, 30625-30639, 10.1029/1999jd900391, 1999.

Guenther, A., Karl, T., Harley, P., Wiedinmyer, C., Palmer, P. I., and Geron, C.: Estimates of global terrestrial isoprene emissions using MEGAN (Model of Emissions of Gases and Aerosols from Nature), Atmos. Chem. Phy., 6, 3181-3210, 10.5194/acp-6-3181-2006, 2006.

Guenther, A. B., Zimmerman, P. R., Harley, P. C., Monson, R. K., and Fall, R.: Isoprene and monoterpene emission rate variability - model evaluations and sensitivity analyses, J. Geophys. Res.-Atmos, 98, 12609-12617, 10.1029/93jd00527, 1993.

Guenther, A. B., Jiang, X., Heald, C. L., Sakulyanontvittaya, T., Duhl, T., Emmons, L. K., and Wang, X.: The Model of Emissions of Gases and Aerosols from Nature version 2.1 (MEGAN2.1): an extended and updated framework for modeling biogenic emissions, Geosci. Model Dev., 5, 1471-1492, 10.5194/gmd-5-1471-2012, 2012.

Hallquist, M., Wenger, J. C., Baltensperger, U., Rudich, Y., Simpson, D., Claeys, M., Dommen, J., Donahue, N. M., George, C., Goldstein, A. H., Hamilton, J. F., Herrmann, H., Hoffmann, T., Iinuma, Y., Jang, M., Jenkin, M. E., Jimenez, J. L., Kiendler-Scharr, A., Maenhaut, W., McFiggans, G., Mentel, T. F., Monod, A., Prévôt, A. S. H., Seinfeld, J. H., Surratt, J. D., Szmigielski, R., and Wildt, J.: The formation, properties and impact of secondary organic aerosol: current and emerging issues, Atmos. Chem. Phy., 9, 5155-5236, 2009.

Hantson, S., Knorr, W., Schurgers, G., Pugh, T. A. M., and Arneth, A.: Global isoprene and monoterpene emissions under changing climate, vegetation, CO2 and land use, Atmos. Environ., 155, 35-45, 10.1016/j.atmosenv.2017.02.010, 2017.

Hildebrandt, L., Engelhart, G. J., Mohr, C., Kostenidou, E., Lanz, V. A., Bougiatioti, A., DeCarlo, P. F., Prévôt, A. S. H., Baltensperger, U., Mihalopoulos, N., Donahue, N. M., and Pandis, S. N.: Aged organic aerosol in the Eastern Mediterranean: the Finokalia Aerosol Measurement Experiment-2008, Atmos. Chem. Phy., 10, 4167-4186, 10.5194/acp-10-4167-2010, 2010.

Hildebrandt Ruiz, L., and Yarwood, G.: Interactions between organic aerosol and NOy: Influence on oxidant production., University of Texas at Austin, and ENVIRON International Corporation, Novato, CA, 2013.

Hodzic, A., Kasibhatla, P. S., Jo, D. S., Cappa, C. D., Jimenez, J. L., Madronich, S., and Park, R. J.: Rethinking the global secondary organic aerosol (SOA) budget: stronger production, faster removal, shorter lifetime, Atmos. Chem. Phy., 16, 7917-7941, 10.5194/acp-16-7917-2016, 2016.

Hoffmann, T., Odum, J. R., Bowman, F., Collins, D., Klockow, D., Flagan, R. C., and Seinfeld, J. H.: Formation of organic aerosols from the oxidation of biogenic hydrocarbons, J. Atmos. Chem, 26, 189-222, 10.1023/a:1005734301837, 1997.

Horowitz, L. W., Walters, S., Mauzerall, D. L., Emmons, L. K., Rasch, P. J., Granier, C., Tie, X. X., Lamarque, J. F., Schultz, M. G., Tyndall, G. S., Orlando, J. J., and Brasseur, G. P.: A global simulation of

© Author(s) 2018. CC BY 4.0 License.

tropospheric ozone and related tracers: Description and evaluation of MOZART, version 2, J. Geophys. Res.-Atmos, 108, 10.1029/2002jd002853, 2003.

Hoyle, C. R., Boy, M., Donahue, N. M., Fry, J. L., Glasius, M., Guenther, A., Hallar, A. G., Huff Hartz, K., Petters, M. D., Petäjä, T., Rosenoern, T., and Sullivan, A. P.: A review of the anthropogenic influence on biogenic secondary organic aerosol, Atmos. Chem. Phy., 11, 321-343, 10.5194/acp-11-321-2011, 2011.

Im, U., Bianconi, R., Solazzo, E., Kioutsioukis, I., Badia, A., Balzarini, A., Baro, R., Bellasio, R., Brunner, D., Chemel, C., Curci, G., Flemming, J., Forkel, R., Giordano, L., Jimenez-Guerrero, P., Hirtl, M., Hodzic, A., Honzak, L., Jorba, O., Knote, C., Kuenen, J. J. P., Makar, P. A., Manders-Groot, A., Neal, L., Perez, J. L., Pirovano, G., Pouliot, G., San Jose, R., Savage, N., Schroder, W., Sokhi, R. S., Syrakov, D., Torian, A., Tuccella, P., Werhahn, J., Wolke, R., Yahya, K., Zabkar, R., Zhang, Y., Zhang, J., Hogrefe, C., and Galmarini, S.: Evaluation of operational on-line-coupled regional air quality models over Europe and North America in the context of AQMEII phase 2. Part I: Ozone, Atmos. Environ., 115, 404-420, 10.1016/j.atmosenv.2014.09.042, 2015.

Joss, U.: Mikrometereologie, Profile und Flüsse von CO2, H2O, NO2, O3 in zwei mitteleuropäischen Nadelwäldern, PhD, University of Basel, Basel, Switzerland, 1995.

Keller, A., Andreani-aksoyoglu, S., and Joss, U.: Inventory of natural emissions in Switzerland, in: Air Pollution III, Volume 2, Air Pollution Engineering and Management, edited by: Power, H., Moussiopoulos, N., Brebbia C.A, Computational Mechanics Publications, Southampton, UK, 339-346, 1995.

Kesselmeier, J., and Staudt, M.: Biogenic Volatile Organic Compounds (VOC): An Overview on Emission, Physiology and Ecology, J. Atmos. Chem, 33, 23-88, 10.1023/a:1006127516791, 1999.

Kiendler-Scharr, A., Mensah, A. A., Friese, E., Topping, D., Nemitz, E., Prévôt, A. S. H., Aijala, M., Allan, J., Canonaco, F., Canagaratna, M., Carbone, S., Crippa, M., Dall Osto, M., Day, D. A., De Carlo, P., Di Marco, C. F., Elbern, H., Eriksson, A., Freney, E., Hao, L., Herrmann, H., Hildebrandt, L., Hillamo, R., Jimenez, J. L., Laaksonen, A., McFiggans, G., Mohr, C., O'Dowd, C., Otjes, R., Ovadnevaite, J., Pandis, S. N., Poulain, L., Schlag, P., Sellegri, K., Swietlicki, E., Tiitta, P., Vermeulen, A., Wahner, A., Worsnop, D., and Wu, H. C.: Ubiquity of organic nitrates from nighttime chemistry in the European submicron aerosol, Geophys. Res. Lett., 43, 7735-7744, 10.1002/2016gl069239, 2016.

Kim, E., Kim, B. U., Kim, H. C., and Kim, S.: The Variability of Ozone Sensitivity to Anthropogenic Emissions with Biogenic Emissions Modeled by MEGAN and BEIS3, Atmos, 8, 24, 10.3390/atmos8100187, 2017.

Koo, B., Knipping, E., and Yarwood, G.: 1.5-Dimensional volatility basis set approach for modeling organic aerosol in CAMx and CMAQ, Atmos. Environ., 95, 158-164, 10.1016/j.atmosenv.2014.06.031, 2014.

Kuenen, J. J. P., Visschedijk, A. J. H., Jozwicka, M., and Denier van der Gon, H. A. C.: TNO-MACC_II emission inventory; a multi-year (2003–2009) consistent high-resolution European emission inventory for air quality modelling, Atmos. Chem. Phy., 14, 10963-10976, 10.5194/acp-14-10963-2014, 2014.

Lamb, B., Gay, D., Westberg, H., and Pierce, T.: A biogenic hydrocarbon emission inventory for the U.S.A. using a simple forest canopy model, Atmos. Environ. Part A, 27, 1673-1690, 10.1016/0960-1686(93)90230-V, 1993.

Li, G. H., Zhang, R. Y., Fan, J. W., and Tie, X. X.: Impacts of biogenic emissions on photochemical ozone production in Houston, Texas, J. Geophys. Res.-Atmos, 112, 10.1029/2006jd007924, 2007.

Megaritis, A. G., Fountoukis, C., Charalampidis, P. E., Pilinis, C., and Pandis, S. N.: Response of fine particulate matter concentrations to changes of emissions and temperature in Europe, Atmos. Chem. Phy., 13, 3423-3443, 10.5194/acp-13-3423-2013, 2013.

Messina, P., Lathiere, J., Sindelarova, K., Vuichard, N., Granier, C., Ghattas, J., Cozic, A., and Hauglustaine, D. A.: Global biogenic volatile organic compound emissions in the ORCHIDEE and MEGAN models and sensitivity to key parameters, Atmos. Chem. Phy., 16, 14169-14202, 10.5194/acp-16-14169-2016, 2016.

Mol, W., and Leeuw, F.: AirBase: a valuable tool in air quality assessments, Proceedings of the 5th International Conference on Urban Air Quality, Valencia, Spain, 2005.

NCAR: The Tropospheric Visible and Ultraviolet (TUV) Radiation Model web page, National Center for Atmospheric Research, Atmospheric Chemistry Division, Boulder, Colorado, 2011.

NCAR: Weather Research and Forecasting Model WRF-ARW Version 3 Modeling System User's Guide, National Center for Atmospheric Research, Boulder, Colorado, USA, 2016.

Nenes, A., Pandis, S. N., and Pilinis, C.: ISORROPIA: A new thermodynamic equilibrium model for multiphase multicomponent inorganic aerosols, Aquat. Geochem., 4, 123-152, 10.1023/a:1009604003981, 1998.

Ng, N. L., Brown, S. S., Archibald, A. T., Atlas, E., Cohen, R. C., Crowley, J. N., Day, D. A., Donahue, N. M., Fry, J. L., Fuchs, H., Griffin, R. J., Guzman, M. I., Herrmann, H., Hodzic, A., Iinuma, Y., Jimenez, J. L., Kiendler-Scharr, A., Lee, B. H., Luecken, D. J., Mao, J. Q., McLaren, R., Mutzel, A., Osthoff, H. D., Ouyang, B., Picquet-Varrault, B., Platt, U., Pye, H. O. T., Rudich, Y., Schwantes, R. H., Shiraiwa, M., Stutz, J., Thornton, J. A., Tilgner, A., Williams, B. J., and Zaveri, R. A.: Nitrate radicals and biogenic

© Author(s) 2018. CC BY 4.0 License.

volatile organic compounds: oxidation, mechanisms, and organic aerosol, Atmos. Chem. Phy., 17, 2103-2162, 10.5194/acp-17-2103-2017, 2017.

O'Dowd, C., Ceburnis, D., Ovadnevaite, J., Vaishya, A., Rinaldi, M., and Facchini, M. C.: Do anthropogenic, continental or coastal aerosol sources impact on a marine aerosol signature at Mace Head?, Atmos. Chem. Phys., 14, 10687-10704, 10.5194/acp-14-10687-2014, 2014.

Oderbolz, D. C., Aksoyoglu, S., Keller, J., Barmpadimos, I., Steinbrecher, R., Skjøth, C. A., Plaß-Dülmer, C., and Prévôt, A. S. H.: A comprehensive emission inventory of biogenic volatile organic compounds in Europe: improved seasonality and land-cover, Atmos. Chem. Phys., 13, 1689-1712, 10.5194/acp-13-1689-2013, 2013.

Odum, J. R., Hoffmann, T., Bowman, F., Collins, D., Flagan, R. C., and Seinfeld, J. H.: Gas/particle partitioning and secondary organic aerosol yields, Environ. Sci. Technol., 30, 2580-2585, 10.1021/es950943+, 1996.

Oikonomakis, E., Aksoyoglu, S., Ciarelli, G., Baltensperger, U., and Prévôt, A. S. H.: Low modeled ozone production suggests underestimation of precursor emissions (especially NOx) in Europe, Atmos. Chem. Phys., 18, 2175-2198, 10.5194/acp-18-2175-2018, 2018.

Ovadnevaite, J., Ceburnis, D., Leinert, S., Dall'Osto, M., Canagaratna, M., O'Doherty, S., Berresheim, H., and O'Dowd, C.: Submicron NE Atlantic marine aerosol chemical composition and abundance: Seasonal trends and air mass categorization, J. Geophys. Res.-Atmos, 119, 11850-11863, 10.1002/2013jd021330, 2014.

Passant, N. R.: Speciation of UK emissions of non-methane volatile organic compounds, AEA Technology, Culham, Abingdon, Oxon, UK, 2002.

Petit, J. E., Favez, O., Sciare, J., Crenn, V., Sarda-Esteve, R., Bonnaire, N., Mocnik, G., Dupont, J. C., Haeffelin, M., and Leoz-Garziandia, E.: Two years of near real-time chemical composition of submicron aerosols in the region of Paris using an Aerosol Chemical Speciation Monitor (ACSM) and a multi-wavelength Aethalometer, Atmos. Chem. Phy., 15, 2985-3005, 10.5194/acp-15-2985-2015, 2015.

Poupkou, A., Giannaros, T., Markakis, K., Kioutsioukis, I., Curci, G., Melas, D., and Zerefos, C.: A model for European Biogenic Volatile Organic Compound emissions: Software development and first validation, Environ. Modell. Softw., 25, 1845-1856, 10.1016/j.envsoft.2010.05.004, 2010.

Ripoll, A., Minguillón, M. C., Pey, J., Jimenez, J. L., Day, D. A., Sosedova, Y., Canonaco, F., Prévôt, A. S. H., Querol, X., and Alastuey, A.: Long-term real-time chemical characterization of submicron aerosols at Montsec (southern Pyrenees, 1570 m a.s.l.), Atmos. Chem. Phys., 15, 2935-2951, 10.5194/acp-15-2935-2015, 2015.

Rosenkranz, M., Pugh, T. A. M., Schnitzler, J. P., and Arneth, A.: Effect of land-use change and management on biogenic volatile organic compound emissions - selecting climate-smart cultivars, Plant Cell Environ., 38, 1896-1912, 10.1111/pce.12453, 2015.

Sartelet, K. N., Couvidat, F., Seigneur, C., and Roustan, Y.: Impact of biogenic emissions on air quality over Europe and North America, Atmos. Environ., 53, 131-141, 10.1016/j.atmosenv.2011.10.046, 2012.

Satoo, T., and Madgwick, H. A.: Forest Biomass, Martinus Nijhoff/Dr W. Junk Publishers, The Hague, 1982.

Schmale, J., Henning, S., Henzing, B., Keskinen, H., Sellegri, K., Ovadnevaite, J., Bougiatioti, A., Kalivitis, N., Stavroulas, I., Jefferson, A., Park, M., Schlag, P., Kristensson, A., Iwamoto, Y., Pringle, K., Reddington, C., Aalto, P., Äijälä, M., Baltensperger, U., Bialek, J., Birmili, W., Bukowiecki, N., Ehn, M., Fjæraa, A. M., Fiebig, M., Frank, G., Fröhlich, R., Frumau, A., Furuya, M., Hammer, E., Heikkinen, L., Herrmann, E., Holzinger, R., Hyono, H., Kanakidou, M., Kiendler-Scharr, A., Kinouchi, K., Kos, G., Kulmala, M., Mihalopoulos, N., Motos, G., Nenes, A., O'Dowd, C., Paramonov, M., Petäjä, T., Picard, D., Poulain, L., Prévôt, A. S. H., Slowik, J., Sonntag, A., Swietlicki, E., Svenningsson, B., Tsurumaru, H., Wiedensohler, A., Wittbom, C., Ogren, J. A., Matsuki, A., Yum, S. S., Myhre, C. L., Carslaw, K., Stratmann, F., and Gysel, M.: Collocated observations of cloud condensation nuclei, particle size distributions, and chemical composition, Sci. Data, 4, 170003, 10.1038/sdata.2017.3, 2017.

Schürmann, W.: Emission von Monoterpenen aus Nadeln von Picea Abies (L.) Karst, sowie deren Verhalten in der Atmosphäre, PhD, Technische Universität München, 1993.

Silibello, C., Baraldi, R., Rapparini, F., Facini, O., Neri, L., Brilli, F., Fares, S., Finardi, S., Magliulo, E., Ciccioli, P., and Ciccioli, P.: Modelling of biogenic volatile organic compounds emissions over italy, 18th International Conference on Harmonisation within Atmospheric Dispersion Modelling for Regulatory Purposes (HARMO), Bologna, Italy, 2017.

Simpson, D., Winiwarter, W., Borjesson, G., Cinderby, S., Ferreiro, A., Guenther, A., Hewitt, C. N., Janson, R., Khalil, M. A. K., Owen, S., Pierce, T. E., Puxbaum, H., Shearer, M., Skiba, U., Steinbrecher, R., Tarrason, L., and Oquist, M. G.: Inventorying emissions from nature in Europe, J. Geophys. Res.-Atmos, 104, 8113-8152, 10.1029/98jd02747, 1999.

Sindelarova, K., Granier, C., Bouarar, I., Guenther, A., Tilmes, S., Stavrakou, T., Müller, J. F., Kuhn, U., Stefani, P., and Knorr, W.: Global data set of biogenic VOC emissions calculated by the MEGAN model over the last 30 years, Atmos. Chem. Phy., 14, 9317-9341, 10.5194/acp-14-9317-2014, 2014.

© Author(s) 2018. CC BY 4.0 License.

Skamarock, W. C., Klemp, J. B., Dudhia, J., Gill, D. O., Barker, D. M., Duda, M. G., Huang, X.-Y., Wang, W., and Powers, J. G.: A Description of the Advanced Research WRF Version 3, Mesoscale and Microscale Meteorology Division, National Center for Atmospheric Research, Boulder, Colorado, USA, 2008.

Solazzo, E., Bianconi, R., Pirovano, G., Matthias, V., Vautard, R., Moran, M. D., Appel, K. W., Bessagnet, B., Brandt, J., Christensen, J. H., Chemel, C., Coll, I., Ferreira, J., Forkel, R., Francis, X. V., Grell, G., Grossi, P., Hansen, A. B., Miranda, A. I., Nopmongcol, U., Prank, M., Sartelet, K. N., Schaap, M., Silver, J. D., Sokhi, R. S., Vira, J., Werhahn, J., Wolke, R., Yarwood, G., Zhang, J. H., Rao, S. T., and Galmarini, S.: Operational model evaluation for particulate matter in Europe and North America in the context of AQMEII, Atmos. Environ., 53, 75-92, 10.1016/j.atmosenv.2012.02.045, 2012.

Solazzo, E., Bianconi, R., Hogrefe, C., Curci, G., Tuccella, P., Alyuz, U., Balzarini, A., Baro, R., Bellasio, R., Bieser, J., Brandt, J., Christensen, J. H., Colette, A., Francis, X., Fraser, A., Vivanco, M. G., Jimenez-Guerrero, P., Im, U., Manders, A., Nopmongcol, U., Kitwiroon, N., Pirovano, G., Pozzoli, L., Prank, M., Sokhi, R. S., Unal, A., Yarwood, G., and Galmarini, S.: Evaluation and error apportionment of an ensemble of atmospheric chemistry transport modeling systems: multivariable temporal and spatial breakdown, Atmos. Chem. Phy., 17, 3001-3054, 10.5194/acp-17-3001-2017, 2017.

Solmon, F., Sarrat, C., Serca, D., Tulet, P., and Rosset, R.: Isoprene and monoterpenes biogenic emissions in France: modeling and impact during a regional pollution episode, Atmos. Environ., 38, 3853-3865, 10.1016/j.atmosenv.2004.03.054, 2004.

Stein, A. F., Draxler, R. R., Rolph, G. D., Stunder, B. J. B., Cohen, M. D., and Ngan, F.: Noaa's hysplit atmospheric transport and dispersion modeling system, Bull. Am. Meteorol. Soc., 96, 2059-2077, 10.1175/bams-d-14-00110.1, 2015.

Steinbrecher, R., Smiatek, G., Koble, R., Seufert, G., Theloke, J., Hauff, K., Ciccioli, P., Vautard, R., and Curci, G.: Intra- and inter-annual variability of VOC emissions from natural and semi-natural vegetation in Europe and neighbouring countries, Atmos. Environ., 43, 1380-1391, 10.1016/j.atmosenv.2008.09.072, 2009.

Szogs, S., Arneth, A., Anthoni, P., Doelman, J. C., Humpenoder, F., Popp, A., Pugh, T. A. M., and Stehfest, E.: Impact of LULCC on the emission of SVOCs during the 21st century, Atmos. Environ., 165, 73-87, 10.1016/j.atmosenv.2017.06.025, 2017.

Tingey, D. T., Manning, M., Grothaus, L. C., and Burns, W. F.: Influence of light and temperature on monoterpene emission rates from slash pine, Plant Physiology, 65, 797-801, 10.1104/pp.65.5.797, 1980.

van Der Gon, H. D.: TNO-MACC_III emission high resolution emission inventory and a small excursion to source apportionment, MACC policy workshop, Vienna, 2015.

Wen, L., Chen, J., Yang, L., Wang, X., Caihong, X., Sui, X., Yao, L., Zhu, Y., Zhang, J., Zhu, T., and Wang, W.: Enhanced formation of fine particulate nitrate at a rural site on the North China Plain in summer: The important roles of ammonia and ozone, Atmos. Environ., 101, 294-302, doi.org/10.1016/j.atmosenv.2014.11.037, 2015.

Wennberg, P. O., Bates, K. H., Crounse, J. D., Dodson, L. G., McVay, R. C., Mertens, L. A., Nguyen, T. B., Praske, E., Schwantes, R. H., Smarte, M. D., St Clair, J. M., Teng, A. P., Zhang, X., and Seinfeld, J. H.: Gas-Phase Reactions of Isoprene and Its Major Oxidation Products, Chem. Rev., 10.1021/acs.chemrev.7b00439, 2018.

Zare, A., Christensen, J. H., Irannejad, P., and Brandt, J.: Evaluation of two isoprene emission models for use in a long-range air pollution model, Atmos. Chem. Phy., 12, 7399-7412, 10.5194/acp-12-7399-2012, 2012.

Zhang, R., Cohan, A., Biazar, A. P., and Cohan, D. S.: Source apportionment of biogenic contributions to ozone formation over the United States, Atmos. Environ., 164, 8-19, 10.1016/j.atmosenv.2017.05.044, 2017.

Atmos. Chem. Phys. Discuss., https://doi.org/10.5194/acp-2018-920
Manuscript under review for journal Atmos. Chem. Phys.
Discussion started: 17 October 2018
© Author(s) 2018. CC BY 4.0 License.

Atmospheric Chemistry and Physics Discussions

Table 1. Comparison between major input of PSI model and MEGAN v2.1

Inputs	**PSI Model**	**MEGAN v2.1**
Meteorology	WRF-ARW v3.7.1	WRF-ARW v3.7.1
Land-use	GlobCover 2006 inventory ($0.00028^{o} \times 0.00028^{o}$) Vegetation class 1. Norway spruce (*Picea abies*) 2. Silver fir (*Abies alba*) 3. Scots pine (*Pinus sylvestris*) 4. Arolla pine (*Pinus cembra*) 5. European larch (*Larix decidua*) 6. European beech (*Fagus sylvatica*) 7. Sycamore maple (*Acer pseudoplanatus*) 8. Common ash (*Fraxinus excelcior*) 9. European oak (*Quercus robur*) 10. Sweet chestnut (*Castanea sativa*) 11. Pasture 12. Crop	Community Land Model version 4 (CLM4, $0.05^{o} \times 0.05^{o}$) Plant Functional Type (PFT) 1. Needleleaf Evergreen Temperate Tree 2. Needleleaf Evergreen Boreal Tree 3. Needleleaf Deciduous Boreal Tree 4. Broadleaf Evergreen Tropical Tree 5. Broadleaf Evergreen Temperate Tree 6. Broadleaf Deciduous Tropical Tree 7. Broadleaf Deciduous Temperate Tree 8. Broadleaf Deciduous Boreal Tree 9. Broadleaf Evergreen Temperate Shrub 10. Broadleaf Deciduous Temperate Shrub 11. Broadleaf Deciduous Boreal Shrub 12. Arctic C3 Grass 13. Cool C3 Grass 14. Warm C4 Grass 15. Crop
Emission factors	Reference emission rate calculated based on Steinbrecher et al (2009) (Unit: $\mu g\ g_{dw}^{-1}\ h^{-1}$)[1]	Global Emission Factors Version 2011 from MEGAN website (Unit: $\mu g\ m^{-2}\ h^{-1}$)
Biomass density	Leaf biomass density (g dry weight per m^2 projected area) of each tree species obtained from Cannell (1982) and Satoo and Madgwick (1982)	TERRA/ MODIS (Moderate Resolution Imaging Spectroradiometer) vegetation data products MOD15A2 ($0.1^{o}*0.1^{o}$)

[1] The *dw* in the unit means dry weight of biomass.

Atmos. Chem. Phys. Discuss., https://doi.org/10.5194/acp-2018-920
Manuscript under review for journal Atmos. Chem. Phys.
Discussion started: 17 October 2018
© Author(s) 2018. CC BY 4.0 License.

Atmospheric Chemistry and Physics Discussions

Table 2. Comparison between modelled and measured mean afternoon (12:00–18:00 UTC) mixing ratios of surface ozone at 537 rural AirBase stations. NE represents Northern Europe, CE Central Europe, and SE Southern Europe. MB – mean bias, ME – mean error, RMSE – root mean square error, MFB – mean fractional bias, MFE – mean fractional error.

Season	Region	MB (ppb)		ME (ppb)		RMSE (ppb)		MFB		MFE	
		PSI	MEGAN	PSI	MEGAN	PSI	MEGAN	PSI	MEGAN	PSI	MEGAN
Winter	NE	-2.09	-2.34	4.85	4.88	6.10	6.13	-0.06	-0.07	0.17	0.17
	CE	3.11	2.75	7.05	6.94	9.56	9.46	0.15	0.13	0.31	0.31
	SE	3.97	4.16	7.08	7.21	9.25	9.40	0.14	0.14	0.22	0.23
	Total	2.93	2.74	6.88	6.85	9.25	9.22	0.13	0.12	0.28	0.27
Summer	NE	4.76	5.27	6.74	6.96	8.62	8.90	0.15	0.16	0.20	0.21
	CE	1.97	2.70	6.55	6.34	8.53	8.33	0.08	0.09	0.18	0.17
	SE	0.68	2.20	6.82	6.80	9.03	9.03	0.04	0.06	0.16	0.15
	Total	1.82	2.76	6.64	6.52	8.68	8.57	0.07	0.09	0.17	0.17

Atmos. Chem. Phys. Discuss., https://doi.org/10.5194/acp-2018-920
Manuscript under review for journal Atmos. Chem. Phys.
Discussion started: 17 October 2018
© Author(s) 2018. CC BY 4.0 License.

Table 3. Statistical analysis of aerosols for different ACSM/AMS stations. MB - mean bias, ME – mean error, RMSE - root mean square error, MFB - mean fractional bias, MFE - mean fractional error.

Species	Stations	Type	Time span (days)	MB (μg m^{-3})		ME (μg m^{-3})		RMSE (μg m^{-3})		MFB		MFE	
				PSI	MEGAN	PSI	MEGAN	PSI	MEGAN	PSI	MEGAN	PSI	MEGAN
OA	Zurich	Urban	Feb – Dec (324)	-1.41	-4.31	3.56	4.51	4.88	5.82	-0.28	-0.73	0.63	0.77
	Bologna	Urban	Nov– Dec (21)	-12.11	-13.17	12.40	13.28	15.68	16.36	-0.89	-0.98	0.93	1.00
	Marseille	Urban	Feb – Mar (24)	-6.13	-6.97	6.18	6.98	8.20	8.95	-1.05	-1.24	1.08	1.24
	Paris	Suburban	Oct – Dec (92)	-6.24	-6.50	6.29	6.53	9.51	9.68	-1.08	-1.15	1.12	1.18
	Mace Head	Rural/Remote	Jan – Oct (328)	-0.09	-0.53	0.44	0.53	1.04	1.25	-0.80	-1.30	1.15	1.30
	San Pietro Capofiume	Rural/Remote	Nov– Dec (18)	-2.75	-4.30	5.29	5.85	6.89	7.77	-0.15	-0.35	0.58	0.61
	Montsec	Rural/Remote	Jul – Dec (171)	-1.93	-2.45	2.00	2.46	2.69	3.20	-1.01	-1.28	1.04	1.24
	Finokalia	Rural/Remote	Sep – Oct (30)	-1.23	-2.48	1.56	2.48	2.20	3.10	-0.55	-0.98	0.71	0.99
PSO_4	Zurich	Urban	Feb – Dec (324)	0.32	0.30	1.47	1.47	3.42	3.42	0.03	0.01	0.58	0.58
	Bologna	Urban	Nov– Dec (21)	-0.10	-0.06	1.92	1.94	2.53	2.54	0.04	0.06	0.60	0.61
	Marseille	Urban	Feb – Mar (24)	0.87	0.87	1.19	1.19	1.55	1.55	0.46	0.46	0.61	0.61
	Paris	Suburban	Oct – Dec (92)	1.47	1.47	1.63	1.63	2.69	2.70	0.75	0.75	0.87	0.87
	Mace Head	Rural/Remote	Jan – Oct (328)	0.75	0.75	0.90	0.90	1.50	1.50	0.66	0.66	0.85	0.85
	San Pietro Capofiume	Rural/Remote	Nov– Dec (18)	2.21	2.26	2.27	2.32	2.95	3.00	0.91	0.93	0.94	0.96
	Montsec	Rural/Remote	Jul – Dec (171)	0.01	-0.01	0.80	0.81	1.19	1.20	0.36	0.34	0.70	0.70
	Finokalia	Rural/Remote	Sep – Oct (30)	-1.96	-1.89	2.45	2.40	3.49	3.45	-0.30	-0.28	0.65	0.64
PNO_3	Zurich	Urban	Feb – Dec (324)	1.88	1.87	2.93	2.95	4.35	4.49	0.52	0.47	0.96	0.92
	Bologna	Urban	Nov– Dec (21)	1.86	1.90	8.83	8.85	10.74	10.75	0.08	0.08	0.72	0.72
	Marseille	Urban	Feb – Mar (24)	1.93	2.01	3.12	3.20	4.03	4.13	0.54	0.55	0.91	0.93
	Paris	Suburban	Oct – Dec (92)	2.14	2.13	2.91	2.91	4.32	4.32	0.76	0.76	1.00	1.00
	Mace Head	Rural/Remote	Jan – Oct (328)	1.07	1.21	1.07	1.21	2.81	3.18	1.46	1.60	1.48	1.62
	San Pietro Capofiume	Rural/Remote	Nov– Dec (18)	7.93	7.85	10.54	10.45	13.12	13.06	0.76	0.75	1.05	1.04
	Montsec	Rural/Remote	Jul – Dec (171)	-0.10	-0.10	0.50	0.50	0.85	0.85	0.08	0.09	1.05	1.06
	Finokalia	Rural/Remote	Sep – Oct (30)	0.31	0.34	0.34	0.37	0.68	0.80	0.61	0.64	0.96	0.99
PNH_4	Zurich	Urban	Feb – Dec (324)	1.05	1.04	1.27	1.27	2.24	2.28	0.61	0.56	0.82	0.79
	Bologna	Urban	Nov– Dec (21)	0.53	0.56	2.81	2.83	3.45	3.46	0.07	0.08	0.64	0.65
	Marseille	Urban	Feb – Mar (24)	0.39	0.41	1.01	1.02	1.34	1.36	0.24	0.25	0.59	0.60
	Paris	Suburban	Oct – Dec (92)	0.90	0.89	1.17	1.17	1.82	1.82	0.44	0.44	0.78	0.78
	Mace Head	Rural/Remote	Jan – Oct (328)	0.44	0.48	0.49	0.53	1.20	1.30	0.33	0.38	1.14	1.19
	San Pietro Capofiume	Ruran/Remote	Nov– Dec (18)	2.74	2.73	3.29	3.27	4.21	4.20	0.76	0.76	0.92	0.91
	Montsec	Ruran/Remote	Jul – Dec (171)	-0.27	-0.28	0.38	0.39	0.60	0.61	-0.32	-0.33	0.63	0.64
	Finokalia	Ruran/Remote	Sep – Oct (30)	-0.47	-0.45	0.66	0.65	0.96	0.94	-0.30	-0.28	0.60	0.59

Atmospheric Chemistry and Physics Discussions
Open Access
EGU

Atmos. Chem. Phys. Discuss., https://doi.org/10.5194/acp-2018-920
Manuscript under review for journal Atmos. Chem. Phys.
Discussion started: 17 October 2018
© Author(s) 2018. CC BY 4.0 License.

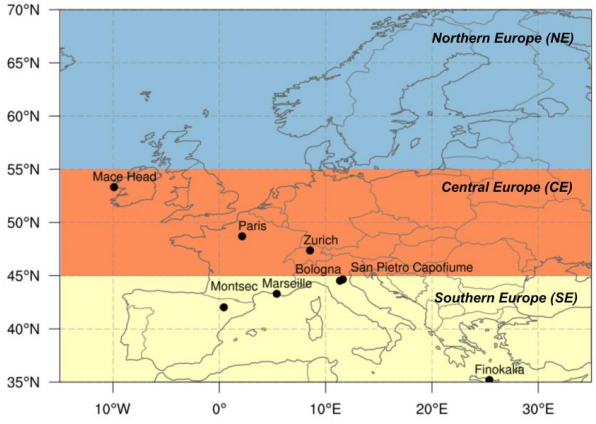

Figure 1. Model domain and location of ACSM/AMS measurement stations.

Atmos. Chem. Phys. Discuss., https://doi.org/10.5194/acp-2018-920
Manuscript under review for journal Atmos. Chem. Phys.
Discussion started: 17 October 2018
© Author(s) 2018. CC BY 4.0 License.

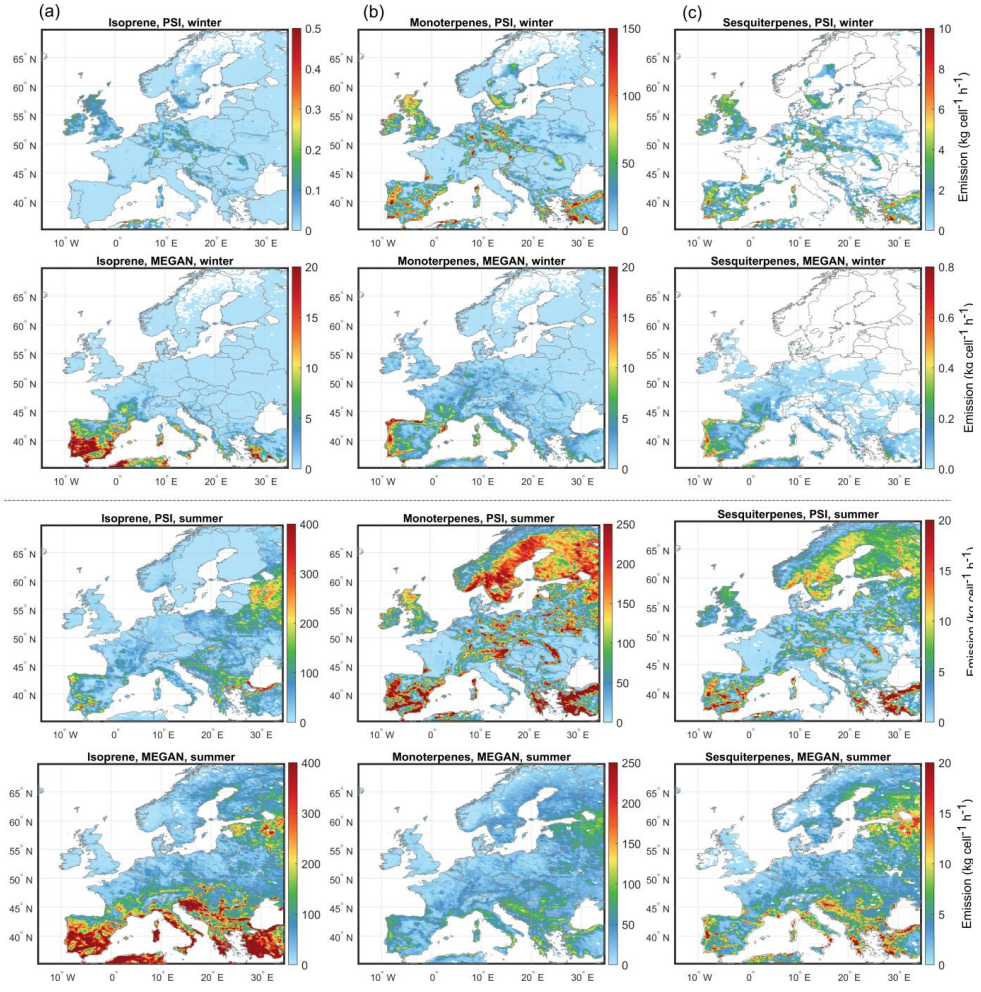

Figure 2. Average hourly emissions of isoprene **(a)**, monoterpenes **(b)** and sesquiterpenes **(c)** estimated by PSI model and MEGAN v2.1. Upper and lower panels represent winter and summer cases, respectively.

Atmos. Chem. Phys. Discuss., https://doi.org/10.5194/acp-2018-920
Manuscript under review for journal Atmos. Chem. Phys.
Discussion started: 17 October 2018
© Author(s) 2018. CC BY 4.0 License.

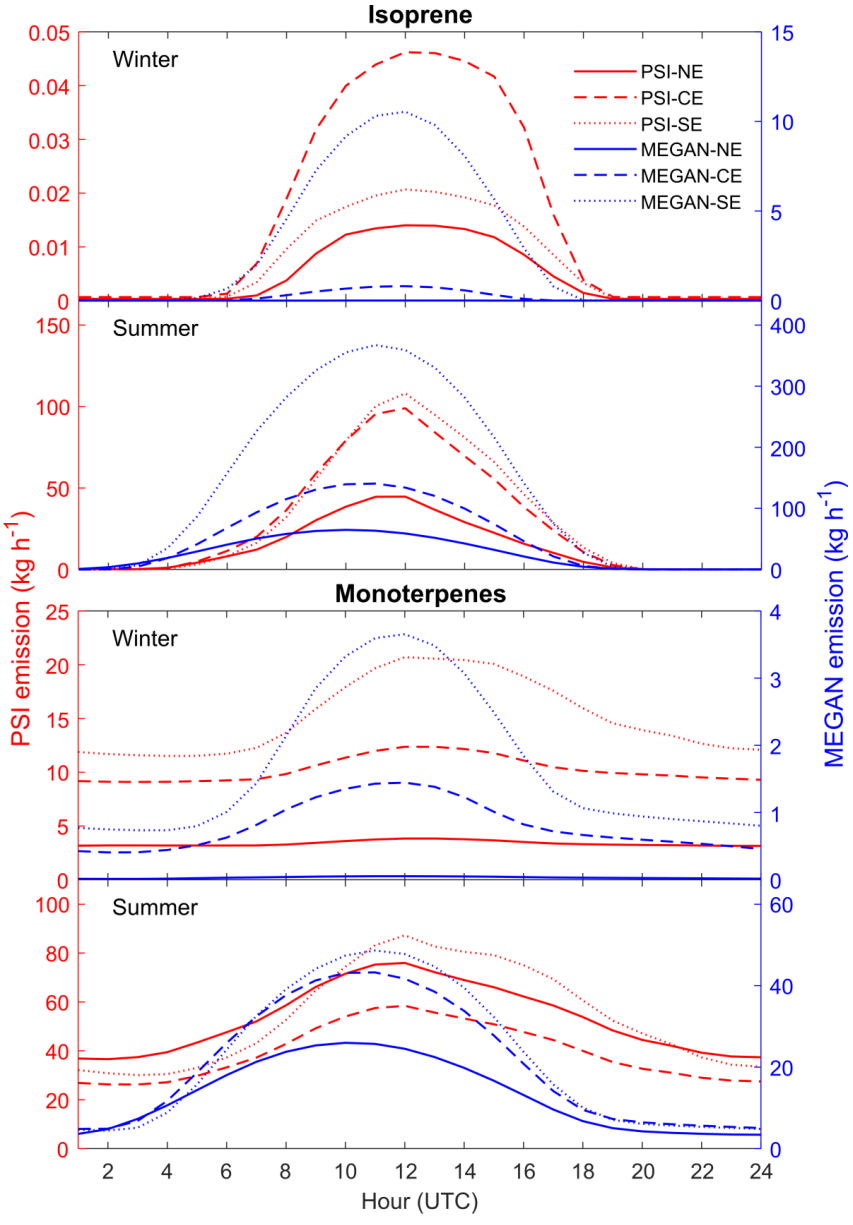

Figure 3. Diurnal variations of isoprene and monoterpene emissions estimated by PSI model (y-axis left) and MEGAN v2.1 (y-axis right). NE represents Northern Europe, CE Central Europe, and SE Southern Europe.

5

Atmos. Chem. Phys. Discuss., https://doi.org/10.5194/acp-2018-920
Manuscript under review for journal Atmos. Chem. Phys.
Discussion started: 17 October 2018
© Author(s) 2018. CC BY 4.0 License.

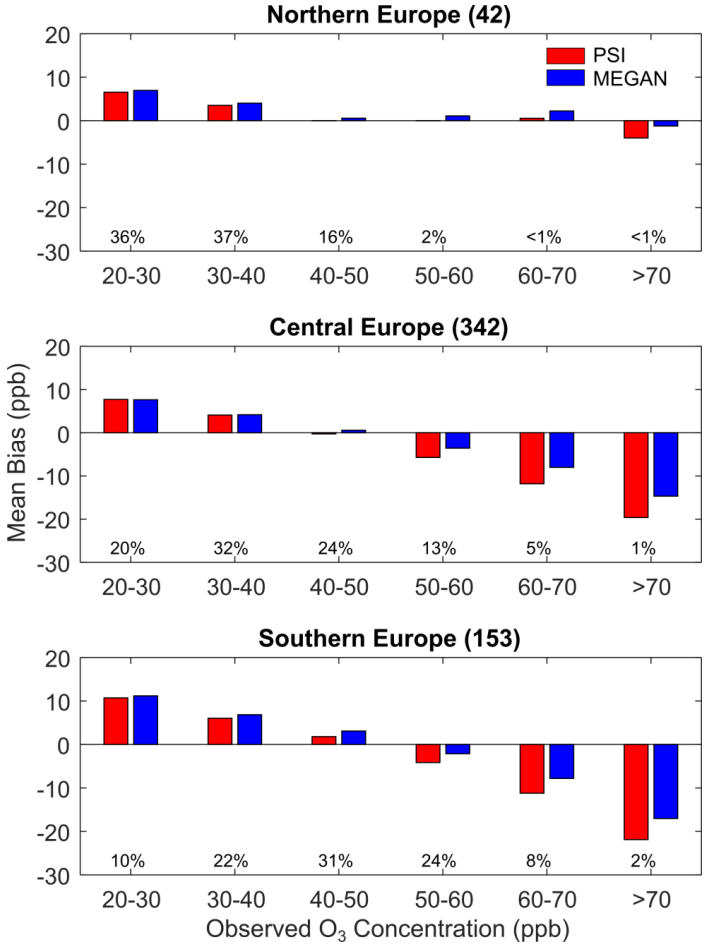

Figure 4. Mean bias of surface O_3 mixing ratios in the afternoon (12:00–18:00 UTC) for each bin of observed ones in July 2011. The number of stations available for each region is reported in parentheses at the top of each panel. Percentage values below the bars show the relative fraction of data in each bin.

Atmos. Chem. Phys. Discuss., https://doi.org/10.5194/acp-2018-920
Manuscript under review for journal Atmos. Chem. Phys.
Discussion started: 17 October 2018
© Author(s) 2018. CC BY 4.0 License.

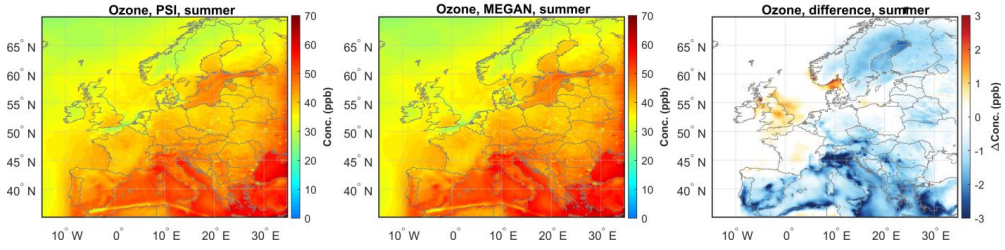

Figure 5. Modelled afternoon (12:00–18:00 UTC) mixing ratios of surface ozone in summer using PSI emissions (O_3-PSI, left), MEGAN emissions (O_3-MEGAN, middle) and the difference between O_3-PSI and O_3-MEGAN (right).

Atmos. Chem. Phys. Discuss., https://doi.org/10.5194/acp-2018-920
Manuscript under review for journal Atmos. Chem. Phys.
Discussion started: 17 October 2018
© Author(s) 2018. CC BY 4.0 License.

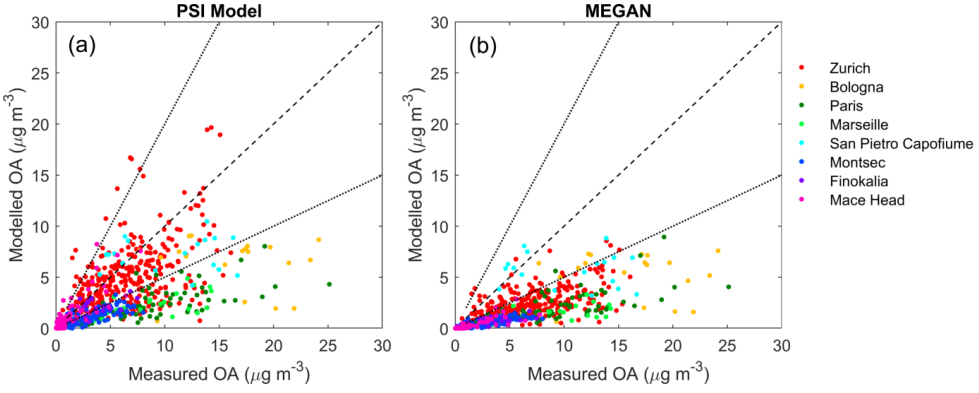

Figure 6. Modelled versus measured daily OA concentrations using BVOC emissions calculated by PSI model (OA-PSI) **(a)** and MEGAN (OA-MEGAN) **(b)** at 8 ACSM/ AMS stations. The dashed line represents 1:1 line, dotted lines represent 2:1 and 1:2 lines.

Atmos. Chem. Phys. Discuss., https://doi.org/10.5194/acp-2018-920
Manuscript under review for journal Atmos. Chem. Phys.
Discussion started: 17 October 2018
© Author(s) 2018. CC BY 4.0 License.

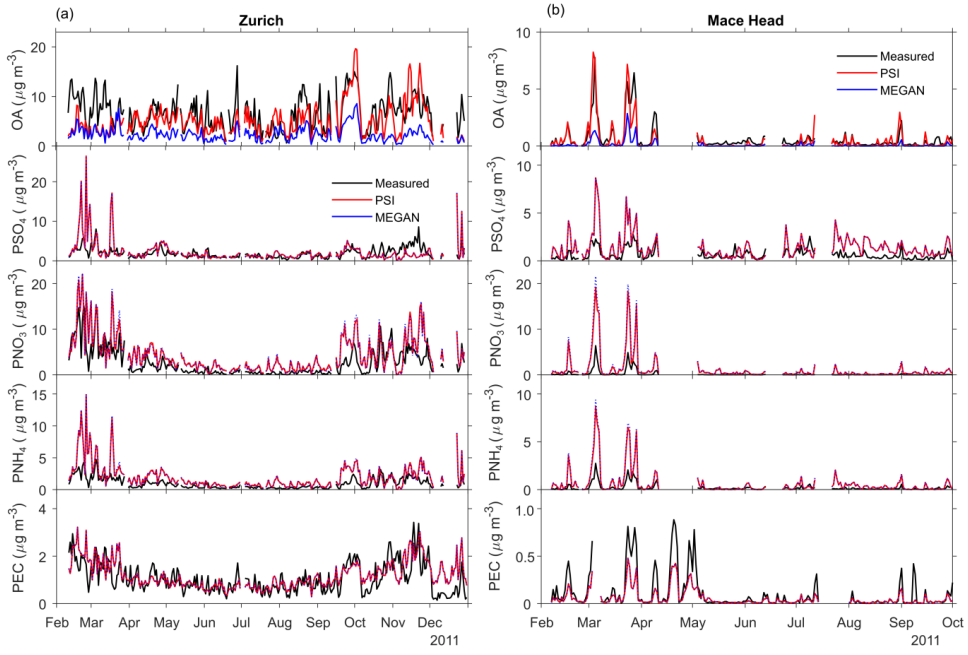

Figure 7. Temporal variation of the modelled (with both PSI and MEGAN emissions) and measured concentrations of organic and inorganic aerosols at Zurich **(a)** and Mace Head **(b)** in 2011.

Atmos. Chem. Phys. Discuss., https://doi.org/10.5194/acp-2018-920
Manuscript under review for journal Atmos. Chem. Phys.
Discussion started: 17 October 2018
© Author(s) 2018. CC BY 4.0 License.

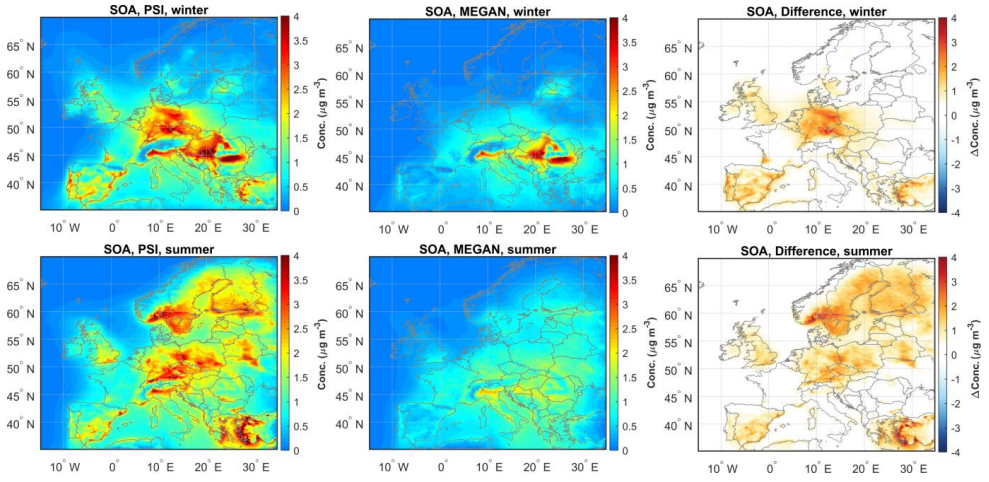

Figure 8. Modelled SOA concentrations using PSI emissions (SOA-PSI) (left), MEGAN emissions (SOA-MEGAN) (middle) and the difference between SOA-PSI and SOA-MEGAN (right).

Atmos. Chem. Phys. Discuss., https://doi.org/10.5194/acp-2018-920
Manuscript under review for journal Atmos. Chem. Phys.
Discussion started: 17 October 2018
© Author(s) 2018. CC BY 4.0 License.

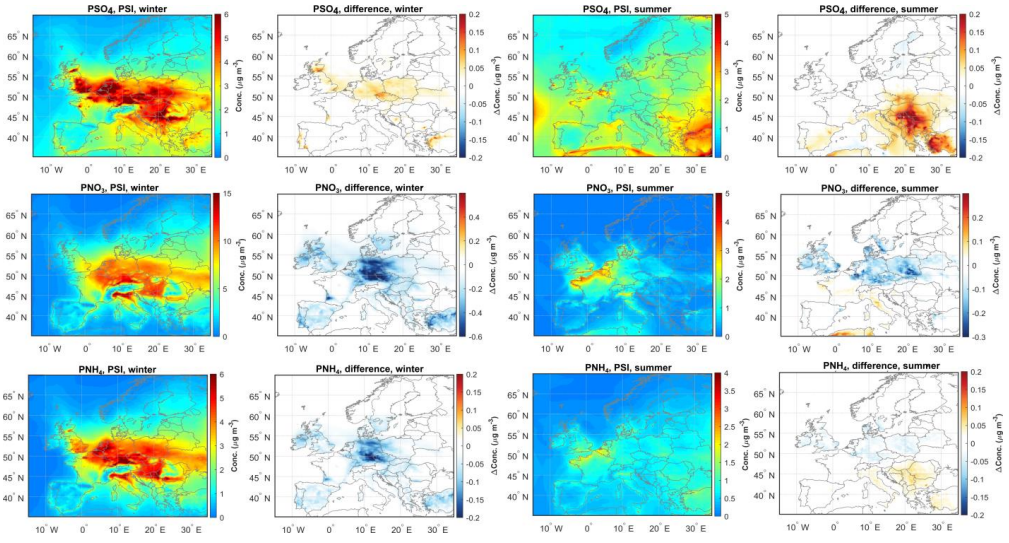

Figure 9. Modelled secondary inorganic aerosol (SIA) concentrations using PSI emissions and the difference between PSI and MEGAN.